

1 An assessment of ocean alkalinity enhancement using aqueous 2 hydroxides: kinetics, efficiency, and precipitation thresholds 3

4 Mallory C. Ringham ¹, Nathan Hirtle ¹, Cody Shaw ¹, Xi Lu ¹, Julian Herndon ^{2,3}, Brendan R. Carter ^{2,3},
5 Matthew D. Eisaman ^{4,5}

6
7 ¹Stony Brook University, Stony Brook, NY, USA

8 ²Cooperative Institute for Climate Ocean and Ecosystem Studies, University of Washington, Seattle, USA

9 ³Pacific Marine Environmental Laboratory, National Oceanic and Atmospheric Administration, Seattle, WA, USA*

10 ⁴Department of Earth & Planetary Sciences, Yale University, New Haven, CT, USA

11 ⁵Yale Center for Natural Carbon Capture, Yale University, New Haven, CT, USA

12 *Coauthors with this affiliation are included provisionally pending institutional manuscript policy review
13

14 Correspondence to: Mallory Ringham (mallory.ringham@stonybrook.edu); Current address: Ebb Carbon Inc., San
15 Carlos, CA, USA

16 Abstract

17 Ocean alkalinity enhancement (OAE) is a promising approach to marine carbon dioxide removal (mCDR) that
18 leverages the large surface area and carbon storage capacity of the oceans to sequester atmospheric CO₂ as dissolved
19 bicarbonate (HCO₃⁻). One OAE method involves the conversion of salt in seawater into aqueous alkalinity (NaOH),
20 which is returned to the ocean. The resulting increase in seawater pH and alkalinity causes a shift in dissolved
21 inorganic carbon (DIC) speciation toward carbonate and a decrease in the surface-ocean pCO₂. The shift in the pCO₂
22 results in enhanced uptake of atmospheric CO₂ uptake by the seawater due to gas exchange. In this study, we
23 systematically test the efficiency of CO₂ uptake in seawater treated with NaOH at aquaria (15L) and tank (6000L)
24 scales to establish operational boundaries for safety and efficiency in advance of scaling up to field experiments.
25 CO₂ equilibration occurred on order of weeks to months, depending on circulation, air forcing, and air bubbling
26 conditions within the test tanks. An increase of ~0.7-0.9 mol DIC/ mol added alkalinity (in the form of NaOH) was
27 observed through analysis of seawater bottle samples and pH sensor data, consistent with the value expected given
28 the values of the carbonate system equilibrium calculations for the range of salinities and temperatures tested.
29 Mineral precipitation occurred when the bulk seawater pH exceeded 10.0 and Ω_{aragonite} exceeded 30.0. This
30 precipitation was dominated by Mg(OH)₂ over hours to 1 day before shifting to CaCO_{3, aragonite} precipitation. These
31 data, combined with models of the dilution and advection of alkaline plumes, will allow for estimation of the
32 amount of carbon dioxide removal expected from OAE pilot studies. Future experiments should better approximate
33 field conditions including sediment interactions, biological activity, ocean circulation, air-sea gas exchange rates,
34 and mixing-zone dynamics.

35 Keywords

36 Ocean Alkalinity Enhancement (OAE); marine carbon dioxide removal (mCDR); ocean carbon dioxide removal
37 (ocean CDR)

39 1 Introduction

40 The Sixth Assessment Report of the Intergovernmental Panel on Climate Change reported that in addition to a
41 drastic decrease in CO₂ emissions, active removal of 5-15 Gt of atmospheric CO₂ per year by 2100 is necessary to

42 constrain average global warming to less than 1.5 - 2 °C (noting that the magnitude of carbon removals varies by
43 climate scenario: IPCC, 2022; Rogelj, 2018). A wide variety of negative emissions technologies (NETs) are under
44 development to meet this enormous challenge (Minx et al., 2018; NASEM, 2019; NASEM, 2021; Rueda et al.,
45 2021; Vitillo et al., 2022).

46 A suite of promising approaches to CO₂ removal termed ocean or marine carbon dioxide removal (ocean CDR or
47 mCDR, respectively) leverage the enormous surface area and carbon storage capacity of the ocean (Boettcher et al.,
48 2019; NASEM, 2021). Ocean alkalinity enhancement (OAE) is an mCDR method that aims to store atmospheric
49 CO₂ in a dissolved phase in the ocean as bicarbonate ions (HCO₃⁻), thereby accelerating a natural planetary CO₂
50 regulation mechanism, the carbonate-silicate cycle (Berner, 1983; Isson et al., 2020). OAE has the potential to scale
51 to gigatons of CO₂ removal per year (He and Tyka, 2023), but development of this approach requires careful
52 consideration of: the methods and materials used to source and process alkalinity; the form and method of delivery
53 of alkalinity to the surface ocean (for example, aqueous or solid phase); and selection of appropriate geographic sites
54 for alkalinity dispersal (Oschlies et al., 2023). OAE methods under exploration include: mining and crushing
55 alkaline minerals (e.g., olivine, basalts) to be spread via ship or in coastal environments (e.g., beach restoration, or
56 salt marsh distribution) (Feng et al., 2017; Köhler, Hartmann, and Wolf-Gladrow, 2010; Monserrat et al., 2018;
57 Rigopoulos et al., 2018); the mining or industrial production of Mg(OH)₂ or mining CaCO₃ and calcining it to CaO
58 or Ca(OH)₂, with the Mg(OH)₂ or Ca(OH)₂ spread via ship or coastal outfall pipe (Harvey, 2008; Ilyina et al., 2013;
59 Khesghi, 1995; La Plante, 2023; Moras et al., 2022; Nduagu, 2012; Rau, 2008; Renforth and Henderson, 2017;
60 Shaw, 2022); and the electrochemical conversion of saltwater into aqueous hydroxides and dispersal via coastal
61 outfalls (de Lannoy et al., 2018; Eisaman et al., 2018; Lu et al., 2022; Tyka, Van Arsdale, and Platt, 2022; Eisaman
62 et al., 2023).

63 Many of these approaches and technologies are at a nascent stage, and we must move quickly to quantitatively
64 test and characterize their performance to determine which, if any, justify larger-scale deployment. The
65 electrochemical conversion of salt (NaCl) into aqueous alkalinity (NaOH) has many potential advantages in scaling
66 considerations, including simplified distribution of a liquid product to the ocean, avoidance of mining and the
67 transportation of the alkalinity source over long distances, and avoidance of potentially harmful impurities present in
68 mined alkalinity sources (NASEM, 2021; Caserini, Storni, and Grosso, 2022).

69 Total alkalinity (TA) is defined as the excess of proton acceptors over proton donors in an aqueous solution (Eq. 1),
70 where ellipses represent neglected acids and bases (Dickson 1981; Dickson 1992; Wolf-Gladrow et al., 2007). A
71 higher TA value for a seawater sample indicates that it has a higher buffering capacity than a sample with a lower
72 TA value. That is, for sample with a higher TA value, the addition of a given amount of acid to the sample will
73 decrease its pH less than for a sample with a lower TA value.

$$74 \quad \text{TA} = [\text{HCO}_3^-] + 2 [\text{CO}_3^{2-}] + [\text{B}(\text{OH})_4^-] + [\text{OH}^-] + [\text{HPO}_4^{2-}] + 2 [\text{PO}_4^{3-}] + \dots - [\text{H}^+] - [\text{HSO}_4^-] - \dots \quad (1)$$

75 From Eq. (1), we see the increased OH⁻ concentration in a treated seawater solution corresponds to a salt solution
76 with increased alkalinity relative to the starting salt solution. This increase in OH⁻ ion concentration rapidly
77 increases the seawater pH upon mixing, resulting in a shift of the dissolved inorganic carbon (DIC) speciation
78 towards carbonate (Eisaman et al., 2023):



81 The concentration of dissolved CO₂ gas (CO_{2,aq}) in this alkalinity-enhanced seawater is less than it would be if it
82 were in equilibrium with atmospheric CO₂ (Equation 2b). Over the longer timescale required for air-sea gas
83 exchange - weeks to months (Wang et al., 2023) or months to years (He and Tyka, 2023) depending on location - the
84 disequilibrium in the surface ocean resulting from the alkalinity addition drives the invasion of atmospheric CO₂

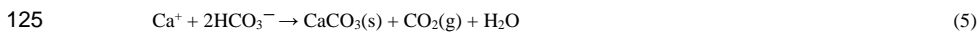
85 into seawater (or lessens the outgassing of CO₂ from the surface ocean to the atmosphere), where it reacts with
86 carbonate and is stored primarily in the stable bicarbonate phase (Jones et al., 2014; Bach et al., 2023; Renforth and
87 Henderson, 2017; Eisaman et al., 2023).



90 Under typical ocean conditions, after equilibrium has been reached, OAE results in an increase in the DIC in
91 seawater on the order of 0.7-0.9 moles of DIC per mole of NaOH added, with a slightly increased pH relative to the
92 initial value (He and Tyka, 2023).

93 It is possible that air-sea gas exchange will not completely drive the seawater pCO₂ to the initial unperturbed value
94 before the seawater sinks into the ocean interior and loses contact with the atmosphere for hundreds to thousands of
95 years. Therefore, the DIC anomaly relative to the alkalinity anomaly present when the seawater sinks into the ocean
96 interior may be used to assess the effective impact of the OAE for capturing atmospheric CO₂ on the 0-100 year
97 timescales that are most important for climate interventions.

98 In addition to the storage of atmospheric CO₂ in the form of DIC, this process may have the potential to locally and
99 transiently mitigate the elevated pCO₂ associated with ocean acidification (NASEM, 2021; Cross et al., 2023;
100 Butenschön et al., 2021). In a water body with a finite seawater exchange rate with the ocean, such as a semi-
101 protected estuary or bay, alkalinity could be added in a controlled manner such that the combination of the rapid
102 reactions described by Eq.(1) and the exchange/flushing rate with the open ocean result in the bay being held in
103 steady-state at a target pH or aragonite saturation state value that is higher than its equilibrium value under
104 conditions of ocean acidification. As this added alkalinity diffuses through the bay and makes its way to the open
105 ocean, CO₂ removal and storage as DIC would occur. By metering the rate of alkalinity addition to the bay to match
106 the flushing rate, the pH or saturation state of the bay can be held at a constant target value. Even once equilibrium
107 has been achieved in the open ocean, the pH and the carbonate ion concentration in the open ocean remains slightly
108 higher than before the alkaline discharge. However, the absolute value of this pH increase after equilibrium has been
109 reached is sufficiently small relative to the alkalinity and DIC increase that mitigating ocean acidification on a
110 global scale with this method is unfeasible. For example, increasing the equilibrium pH value from 8.0 to 8.1 at a
111 fixed pCO₂ of 400 μatm (at 20 C and 35 salinity with no macronutrients) requires a TA increase of around ~620
112 μmol/kg-sw and a DIC increase of around 520 μmol/kg-sw. Using these numbers, mitigating OA over the entire 360
113 million km² surface of the ocean to a depth of 100 meters would require around 487 gigatons of cumulative CO₂
114 removal. Deploying SEA MATE in the ocean or coastal waters will require an understanding of carbonate chemistry
115 in seawater in the ocean volume under consideration, as well as thresholds for safe operation. For example, at the
116 point of alkaline dispersal where there is the maximum change in seawater chemistry, SEA MATE must control the
117 rate of alkalinity addition relative to the rate of mixing and dilution in the ocean to avoid the precipitation of
118 Mg(OH)₂ or CaCO₃ (Hartmann et al., 2023; Moras et al., 2022). While Mg(OH)₂ readily redissolves, an increase in
119 turbidity due to precipitation may negatively affect marine organisms (Bainbridge et al., 2018; Broderon et al.,
120 2017). By contrast, CaCO₃ will generally not redissolve in the surface ocean without biological mediation, and
121 runaway precipitation, where alkalinity removed by precipitation exceeds that added by the OAE treatment, can
122 occur under conditions of increased aragonite saturation state and increased nucleation sites in the water column
123 (Moras et al., 2022). CaCO₃ precipitation could counteract the intended effect of the OAE intervention by removing
124 alkalinity from the surface ocean and releasing CO₂ gas via Eq. 5 (Zeebe and Wolf-Gladrow, 2001):



126 Upon dispersal to the ocean through a coastal outfall pipe, the added alkalinity is advected and diffuses away from
127 the point source, becoming increasingly diluted through the mixing zone. Because the timescale for air-sea gas

128 exchange and re-equilibration described by Eq. (2) is longer than the characteristic timescale for dilution driven by
129 tides, currents, and weather, most of the CO₂ removal occurs far from the mixing zone. Dilution will spread the
130 impacts over a broad area, to an extent that it is unlikely that the impacts on the DIC distribution can be quantified
131 using only direct measurements, given current instrument resolution and the typical dynamic range of natural
132 variability (Wang et al., 2023). In general, options for measurement, reporting, and verification (MRV) of OAE will
133 therefore rely on (Ho et al., 2023): experimentation in laboratory and mesocosm settings, such as the work we
134 describe here, to establish CO₂ removal dynamics under conditions of OAE; direct monitoring of the rate and
135 characteristics of alkalinity addition into seawater; monitoring the seawater carbonate and environmental chemistry
136 in the immediate vicinity of the outfall via sensors and sampling (Cyronak et al., 2023; Schulz et al., 2023); and
137 ocean modeling to estimate CDR beyond the range of direct detection (Fennel et al., 2023).

138 While some work has investigated various aspects of NaOH-based ocean alkalinity enhancement in microcosms
139 (Ferderer et al., 2022; Hartmann et al., 2023), and mesocosms (Groen et al., 2023), and other work has studied the
140 release of NaOH over natural coral reefs as a method of local ocean acidification mitigation (Albright et al., 2016), a
141 systematic characterization of the efficiency and kinetics of OAE as a function of key process parameters has not yet
142 been performed. Here we report the first tank-scale tests of OAE that use aqueous hydroxide (NaOH) to enhance the
143 alkalinity of natural seawater, a process that mimics OAE via the electrochemical brine-to-alkalinity conversion
144 used in the SEA MATE process. Our experiments, conducted in 6,000 liter tanks using seawater pumped from Flax
145 Pond on Long Island Sound in Stony Brook NY, quantify the magnitude and timescale of the CO₂ removal from the
146 air and storage as seawater DIC by monitoring the air-seawater re-equilibration after an initial alkalinity
147 perturbation. In addition, our use of both laboratory-processed bottle samples and field-deployable sensors to
148 measure and over-constrain the carbonate chemistry response allows us to assess the suitability of certain sensing
149 platforms for MRV. Finally, we investigate safe thresholds for the rate and concentration of alkalinity addition to
150 avoid: (1) the precipitation and redissolution of Mg(OH)₂ that can lead to local, temporary increases in turbidity; and
151 (2) the precipitation of CaCO₃, which partially reverses the intended OAE effect by removing alkalinity from, and
152 releasing CO₂ gas into, the surrounding seawater.

153 Using this approach, we address the following key questions:

154 (1) How much additional atmospheric CO₂ is stored in seawater as DIC in response to a given alkalinity
155 perturbation?

156 (2) What is the timescale for CO₂ removal from the air, and how does it depend on pH and the magnitude of
157 alkalinity enhancement?

158 (3) What are the conditions for Mg(OH)₂ precipitation upon addition of NaOH to seawater?

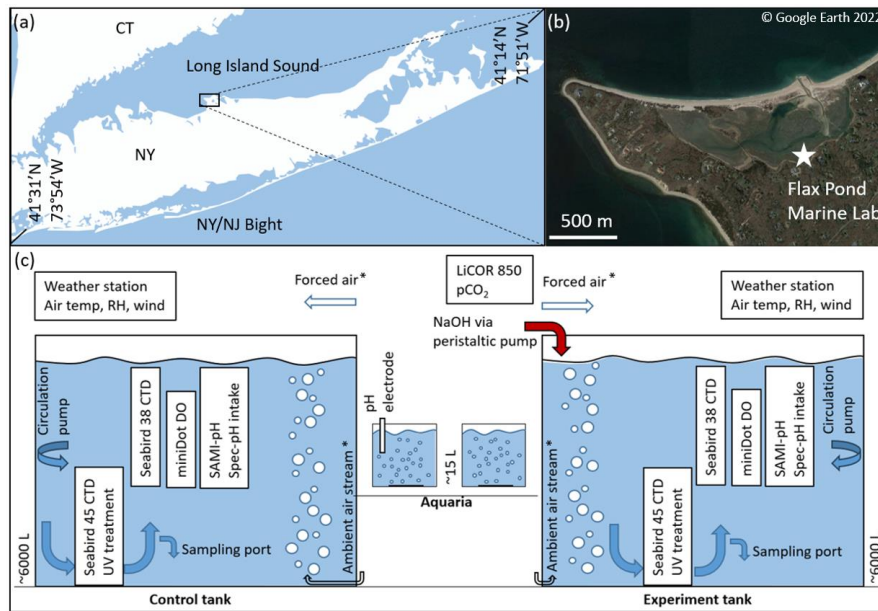
159 (4) What are the threshold values for pH and aragonite saturation state beyond which undesired CaCO₃ precipitation
160 will occur?

161 Answering these questions is key to assessing the viability of this approach and to optimizing its eventual
162 deployment. The large tank experiments presented in this manuscript provide a stepping stone between bench-scale
163 experiments and in-situ mesocosms or field pilots. Even if these experiments simply confirm stoichiometric and
164 modeled expectations, this is critical information in the design and implementation of OAE deployments. This work
165 is a necessary part of the growing scientific body that will allow for field trials to progress.

166 2. Methods

167 2.1 Experimental procedure

168 We investigated the carbonate chemistry changes resulting from the addition of $\text{NaOH}_{(aq)}$ to natural seawater over
 169 timescales ranging from 2 weeks to 2 months in a series of experiments at two scales: (1) two large (~6200 L)
 170 indoor tanks, and (2) multiple 15 L aquaria (Fig. 1). The large volume of tank experiments allowed for precise
 171 measurement of the seawater carbonate chemistry via bottle sampling (1L each, sent to NOAA/PMEL for analysis)
 172 with high sampling frequency. To compliment these measurements, we also performed a series of experiments in
 173 smaller aquaria (15 L each), which enabled a larger number of replicates and a faster time to equilibrium when
 174 bubbled with air.



175
 176 **Figure 1:** (a, b) Flax Pond Marine Laboratory is located on Long Island Sound, New York, USA (© Google Earth
 177 2022). (c) The ~6000 L control and experiment tanks were instrumented with a series of oceanographic sensors and
 178 sampled routinely for DIC/ TA analyses to allow for measurement of carbon uptake over time following an addition
 179 of alkalinity in the form of NaOH. The ~15 L aquaria were instrumented with standard pH electrodes and monitored
 180 with routine TA analyses. The Forced air* and Ambient air streams* indicate their use in some but not all
 181 experiments, as noted in later sections.

182 This study was conducted at the Flax Pond Marine Laboratory at Stony Brook University, NY. All experiments used
 183 natural seawater collected from Flax Pond, part of a 128-acre salt marsh tidal wetlands connected to the Long Island
 184 Sound. The surface areas of the tanks and aquaria were ~4.6 m² and ~0.1 m², respectively. The tanks had a diameter
 185 of 2.4 m, a total height of 1.52 m, and were typically filled to a height of ~1.35 m, allowing for a corresponding
 186 seawater volume of 6185 L. The aquaria had a diameter of 0.3 m and were typically filled to a height of ~0.23 m, for
 187 a total seawater volume of 15 L. The large tank volumes were chosen to limit interactions with walls while
 188 increasing the air-seawater boundary, and to lose a smaller fraction of their volume to evaporation. These tanks
 189 allow for in-situ oceanographic sensor deployment and frequent bottle sampling while retaining semi-controlled
 190 temperature, mixing, filtration, and biological control. The inherent limitations of these tank tests include limited air-
 191 sea interaction, unrealistic light levels and circulation, and biological responses that are not a perfect representation

192 of natural seawater in the ocean, but serve as a stepping stone to mesocosm and eventual field experiments. On
193 average, the large (~6,000 L) tank experiments took ~6.5 weeks after dosing with NaOH to reach 90% of the
194 calculated or extrapolated asymptotic $\Delta\text{DIC}/\text{TA}$ addition ratio indicative of full air-seawater equilibrium, as will be
195 discussed in Section 3. Therefore, in addition to the large tank tests, we conducted a series of smaller aquaria
196 alkalinity additions to increase our capacity for experimental test cases. The limitations of the aquaria include
197 limited sensor options, unrealistic circulation, and limited biological control. While it is expected that equilibration
198 occurs more rapidly in the small aquaria than in the large tanks, the results from these cases should be similar as
199 CO_2 equilibrates across the air-sea boundary. However, we note that some variation is expected due to limited
200 sensing and sampling options in the smaller aquaria and the greater potential for biological growth in the large tanks
201 over longer timescales.

202 2.1.1 Tank experiments

203 Seawater was pumped into the tanks at high tide through a series of sock filters to exclude macroscopic biology. The
204 tanks were then dosed to 40 ppm bleach (sodium hypochlorite) and the shock-treated seawater was allowed to
205 circulate through the tanks for ~1 day to limit biological growth. The seawater was then circulated through UV light
206 arrays to break down the bleach over ~1-2 weeks, as assessed by a standard Hach test kit for free chlorine. During
207 this period, seawater was pumped between the two large test tanks (~25 L/min) to increase mixing of the bleach and
208 to homogenize the tanks to similar initial conditions. For the remainder of each experiment, the seawater was
209 continually pumped through the UV sterilizers. Measurements of total alkalinity showed no significant differences
210 in the bulk seawater TA before and after the bleaching process in any experiment or control tank. In two early
211 experiments (in which bulk pH_T was raised from the initial condition to 8.3 and to 8.7, as described below), the
212 initial pH_T and DIC:TA varied between the control and experiment tanks by 0.17 and 77 $\mu\text{mol kg}^{-1}$, respectively. This
213 was because as seawater was pumped from Flax Pond into multiple reservoirs and was then unevenly distributed
214 between the tanks. The experiments were subsequently refined to allow for several days of cross-pumping between
215 tanks to homogenize the control and experiment seawater before NaOH was added at the start of an experiment.
216 More details on experimental variations and a larger summary table are available in the Supplementary Materials.

217 Oceanographic sensors and discrete daily bottle sampling, as described in Sections 2.2 and 2.3, respectively, were
218 deployed for carbonate chemistry analysis for several days prior to the alkalinity addition to understand the initial
219 baseline conditions in both tanks. Two submerged pumps were used for water circulation within each tank: the first
220 pump (Current eFlux DC Flow Pump, 210 GPH) cycled seawater through the UV arrays with an estimated
221 overturning time of the bulk tank on order of 1 day, and a second (Kedsum Submersible pump, 260 GPH), mounted
222 at an angle halfway down the tank wall, allowed for subsurface circulation within the tank to reduce the occurrence
223 of unmixed 'dead zones' and subsequent non-homogenous biological growth, as assessed visually on the surface of
224 the water and/or tank lining. Initial tank experiments were conducted with a still surface condition, i.e., with no
225 visible water movement across the surface of each tank. As experiments progressed, forced air movement was added
226 across the surface of each tank using a stationary fan with a wind speed of ~5 kph. This was done to control for
227 potential variations in the laboratory HVAC system and to potentially reduce the time to equilibration for the
228 experiments by increasing the rate of air-sea CO_2 equilibration. In later experiments, air was bubbled into the bottom
229 of each tank at a rate of ~30 L min^{-1} with an estimated surface area of ~0.3 m^2 , with a goal of further increasing the
230 rate of equilibration to allow for more rapid throughput of experiments. These variations are further discussed in
231 Section 2.4.

232 After baselining, one tank (referred to as the "experimental tank") was dosed with enough 0.5 M NaOH (see
233 Supplementary Materials) to raise the bulk seawater pH to the target pH of interest for a given experiment, and the
234 same volume of DI water was added to the other tank (referred to as the "control tank"). NaOH additions were
235 typically dosed into the tank via peristaltic pump at a low enough rate (~50 mL/min) that a steady increase in bulk
236 tank pH was observed, but local pH measured just below the NaOH introduction never exceeded a pH of 9.0. A

237 pump (~25 L/min) was placed just below the NaOH stream to speed the mixing of NaOH into the bulk tank,
238 increase dilution from the point source, and to prevent the immediate precipitation of Mg(OH)₂ upon contact of the
239 NaOH with seawater. This pump was removed after the full volume of NaOH was mixed into the tank.

240 After the alkalinity addition, the tanks were left to equilibrate with the atmosphere and were monitored by sensors
241 and sampling as described in Sections 2.2 and 2.3. The tanks were indoors in the wet laboratory at Flax Pond Marine
242 Lab, such that temperature and CO₂ concentration were moderated by the building's HVAC system, but varied
243 throughout days and seasons depending on other uses of the lab space. The experiments were concluded when the
244 observed pH or DIC (calculated from daily pH and frequent TA measurements) appeared to stabilize (e.g., ΔpH
245 ±0.05% or ΔDIC ±10 μmol kg⁻¹ per day) over several days. The continuous improvement of experimental methods
246 during this study resulted in some minor variations among the methods used for each experiment, including methods
247 of NaOH dosing, tank circulation, and biological control, as discussed where necessary in Section 3 and in the
248 Supplementary Materials.

249 2.1.2 Aquaria experiments

250 A series of polycarbonate aquaria were filled with 15 L of seawater taken from the large control tank just after the
251 described bleaching and bleach breakdown procedure was completed. NaOH was dosed into each aquaria to
252 reach a targeted bulk pH_T, with a corresponding volume of DI H₂O added to the control aquaria, and then the
253 seawater was allowed to equilibrate with atmospheric pCO₂ over days to weeks. The aquaria did not have either UV
254 light arrays for biological control or aquarium pumps for internal circulation. ~~With the exception of a single target~~
255 ~~pH_T 8.5 experiment, all aquaria were bubbled with ambient air. In most cases, the aquaria were bubbled with air (~4~~
256 ~~L min⁻¹) via a standard aquarium bubbling bar spanning the center diameter of each aquarium, allowing for rapid~~
257 ~~CO₂ exchange to reduce the equilibration time of these experiments compared to the large tank experiments for all~~
258 ~~initial pH conditions investigated.~~ There was no fine control on air bubbling, but the surface area of all air bubbles in
259 a given aquarium at any point in time was estimated at ~0.01 m². No sensors were deployed in the aquaria due to
260 their limited size, and seawater chemistry was established via discrete pH_T and TA measurements (Sect. 2.2). ~~An~~
261 ~~optically clear lid was placed on each aquarium to reduce evaporation and splashing onto nearby equipment. Some~~
262 ~~evaporation was evident from the rising TA throughout these experiments, but was not resolvable within the~~
263 ~~resolution of a handheld salinometer used for these experiments. Temperature was discretely recorded from a~~
264 ~~combination Ross pH electrode.~~

265 As shown in Eq. (6), we define the dimensionless 'Carbon-to-Alkalinity Ratio' (CAR) for our experiments as the
266 molar ratio of the increase in *n*DIC (in units of μmol/kg, normalized to the system's initial salinity to account for
267 evaporation) to the magnitude of the TA increase (ΔTA, in units of μmol/kg). *n*DIC_{equ} is the measured (via direct
268 titration) or calculated (via CO₂SYS using measured TA and pH_T) DIC value that the system reached at the end of
269 an experiment (Pierrot et al., 2006; Van Heuven et al., 2011). Some experiments were left long enough to achieve
270 equilibration with atmospheric CO₂, but others were halted early. In these cases, a CO₂SYS calculation was used to
271 estimate the DIC increase expected at equilibration given initial seawater conditions, and the difference between this
272 value and the final recorded *n*DIC_{equ} was used to estimate the overall percent equilibration for a given experiment.
273 Depending on experimental constraints described in later sections, *n*DIC_i may represent either: (1) the final *n*DIC
274 measured (via titration of bottle samples) or calculated (via CO₂SYS using seawater TA and pH) in the control tank,
275 or (2) the 'baseline' *n*DIC before the addition of NaOH to a given aquaria experiment, for cases where a
276 corresponding control case may not be available. Note that because we are reporting CAR values where the
277 measured DIC has reached or has been estimated at equilibrium, the CAR values we measure and report reflect the
278 ratio of ΔDIC to ΔTA that would be expected given sufficient time for air-sea exchange to reach equilibrium, and so
279 are equivalent to directly measuring the value of the "TA addition potential impact ratio" as defined by Wang et al.,
280 2023.

281 Carbon-to-Alkalinity Ratio (CAR) = $(n\text{DIC}_{\text{equ}} - n\text{DIC}_i) / \Delta\text{TA}$ (6)

282 **2.2 Oceanographic sensors**

283 Each tank was instrumented with a series of sensors placed halfway down the wall of the tank near the inlet of the
284 UV circulation pump. A Seabird 38 Digital Oceanographic Thermometer and Seabird 45 MicroTSG
285 Thermosalinograph continuously monitored seawater temperature and salinity, respectively. Dissolved oxygen was
286 measured by a PME miniDOT Logger at 10 min resolution. pH_T was monitored daily by a SAMI-pH (manufacturer
287 specified accuracy/precision $\sim 0.003/0.001$, though this accuracy is likely an underestimate of the uncertainty given
288 known challenges for the calibration of the pH_T measurements) and by a semi-automated spectrophotometric (spec-
289 pH) pH unit ($\sim \pm 0.0055/0.0004$) as described by Carter et al. (2013). CRM measurements were taken by each pH
290 system at the beginning and end of each experiment and were used alongside discrete samples of DIC and TA as
291 described in Section 2.3 to constrain the stability of each sensor. The SAMI-pH measurements were recorded at
292 ambient seawater temperature and corrected for in-situ salinity as recorded by the Seabird Thermosalinograph
293 following best practices from the manufacturer. The spec-pH analyses occurred in a jacketed cuvette held at 20 °C
294 (regulated via water bath) and were corrected to the in-situ bulk tank temperature and salinity as recorded by the
295 Seabird Thermometer and Thermosalinograph. Both the SAMI-pH and spec-pH rely on spectrophotometric analysis
296 of metacresol purple indicator dye, which allows for pH measurement within the pH_T range of approximately 7 to 9.
297 For experiments in which enough NaOH was dosed into seawater to raise pH above these limits, a Thermo Scientific
298 Orion ROSS Ultra pH/ATC Triode combination electrode (8157BNUMD) was used to monitor pH_{NBS} at the surface
299 of the tank (± 0.01 precision), which was then converted to pH_T for comparison with the other pH sensor systems.

300 A LiCOR LI-850 sensor was used to analyze atmospheric $p\text{CO}_2$ ($\pm 1.5\%$ accuracy) above the tanks. The inlet to this
301 sensor was periodically moved between tanks to ensure that atmospheric $p\text{CO}_2$ in the vicinity of the control and
302 experiment tanks was the same. AcuRite Iris weather stations were mounted on the side of each tank to monitor air
303 temperature (± 2 °C), relative humidity ($\pm 3\%$), and air speed (± 0.8 m s^{-1}). All data were compiled on an hourly basis
304 in a custom R package.

305 **2.3 Discrete sampling**

306 Two types of discrete sampling were used to constrain carbonate chemistry throughout these experiments. First, 500
307 mL of seawater was collected and preserved from each tank, typically on a daily basis, and as frequently as hourly
308 during the addition of NaOH, following best practices laid out by Dickson (2007) including overflowing of the
309 sample bottles during collection and addition of 0.2 mL of saturated mercuric chloride (HgCl_2) as a preservative.
310 These bottle samples were analyzed for DIC and TA at NOAA Pacific Marine Environmental Laboratory
311 (NOAA/PMEL). DIC concentrations were measured using a coulometer (UIC Inc.) and Single Operator
312 Multiparameter Metabolic Analyzer (SOMMA) (Johnson et al., 1985). TA was determined by an open-cell
313 acidimetric titration (Dickson et al. SOP 3b, 2007). The accuracy of DIC and TA measurements was assessed with
314 Certified Reference Materials (CRMs, supplied by the Dickson laboratory at Scripps Institution of Oceanography),
315 and overall uncertainty for both DIC and TA was typically $\pm 0.1\%$ (~ 2 $\mu\text{mol/kg}$).

316 In addition, discrete seawater samples were analyzed for TA via open-cell potentiometric titration at Stony Brook
317 University. A Thermo Scientific Orion ROSS Ultra pH/ATC Triode combination electrode (8157BNUMD),
318 calibrated using three buffer solutions (pH_{NBS} 4.01, 7, and 10.01) was used to track the titration of a ~ 20 mL
319 seawater sample with a dilute HCl solution (~ 0.1 M in 0.7 M NaCl, calibrated daily with CRM or a secondary
320 seawater standard) following a modified Gran titration procedure using a Kloehe digital syringe pump (Song et al.,
321 2020; Wang and Cai, 2004). The precision of TA measurements was $\sim \pm 5$ -10 $\mu\text{mol/kg}$. This TA data was corrected
322 to that of the bottle samples analyzed via titration at NOAA PMEL where available (see Supplementary Materials).

323 There are several differences between the aquaria experiments and the larger tank experiments. First, the aquaria
324 experiments were monitored daily to every few days by discrete measurement of TA at Stony Brook University and
325 pH_{NBS} via Thermo Scientific Orion ROSS Ultra pH/ATC Triode combination electrode (8157BNUMD) (± 0.01
326 precision), which was then converted to pH_T and corrected against the other pH sensor systems via occasional bottle
327 samples for DIC and TA analysis at NOAA PMEL. Variations between these experiments are noted in Section 3
328 where necessary and in the Supplementary Materials.

329 In either tank or aquaria cases where mineral precipitation was observed, 0.5 – 1 L of seawater was vacuum filtered
330 through a 0.45 μm Whatman GF/F filter via vacuum pump and the solids were rinsed with DI water 3 times to
331 remove NaCl. The precipitate was dried in an oven at 90 °C, then crushed into a uniform powder via mortar and
332 pestle. Samples were analyzed via Hitachi 4800 Scanning Electron Microscopy (SEM) (5 kV) and Rigaku SmartLab
333 X-ray Diffraction (XRD) (Cu $K\alpha$, 1.5406 Å, 10 - 100° 2 θ at 4°/min) at Brookhaven National Laboratory at the
334 Materials Synthesis and Characterization Facility of the Center for Functional Nanomaterials.

335 2.4 Evaluation of CO₂ uptake by seawater in response to NaOH perturbation

336 Seawater carbonate chemistry measurements were used to analyze the uptake of CO₂ in each tank, primarily relying
337 on calculations from the NOAA/PMEL DIC and TA analyses of bottle samples when available and using sensor pH
338 and Stony Brook TA measurements for cross-verification or to fill in between discrete DIC samples. DIC and TA
339 data were normalized to the salinity at the start of a given experiment to account for evaporation (Friis et al., 2003).
340 Carbonate chemistry calculations were then performed using CO2SYS (Lewis and Wallace, 1998), with Lueker et
341 al. (2000) carbonate constants, Dickson (1990) for KSO₄, and Lee et al. (2010) for total boron. Wherever possible, a
342 combination of CRM analyses and comparisons between simultaneous pH sensor and NOAA PMEL bottle samples
343 were used to correct SAMI-pH and spectrophotometric pH sensor data for drift.

344 Changes in the seawater carbonate chemistry over time were analyzed with respect to shifts away from the baseline
345 within a single control or experiment tank, as well as with respect to the differences between the control and
346 experimental tanks.

347 3 Results and Discussion

348 3.1 Large tank experiments

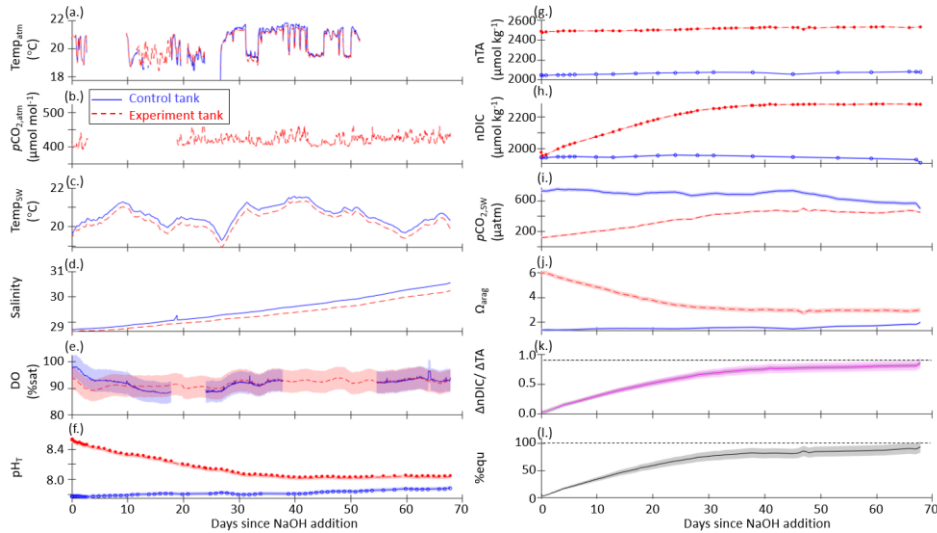
349 A summary of the range of oceanographic variables measured by sensors and bottle samples, calculated via
350 CO2SYS, or extrapolated to equilibration conditions during the large tank experiments is provided in Table 1. This
351 summary includes 6 experiments including 3 targeting pH_T 8.5 (still surface water, with forced air, and with forced
352 air and air bubbling) and one (each) targeting pH_T values of 8.7 (still surface water), 9.5 (with forced air and air
353 bubbling), and 10.3 (still surface water). ~~In two early experiments in which bulk pH_T was raised from the initial
354 condition to 8.3 and to 8.7, the initial pH_T and TA varied between the control and experiment tanks as seawater was
355 pumped from multiple reservoirs and unevenly distributed between the tanks. The experiments were subsequently
356 refined to allow for several days of cross pumping between tanks to homogenize the control and experiment
357 seawater before NaOH was added at the start of an experiment. More details on experimental variations and a larger
358 summary table are available in the Supplementary Materials.~~ While the initial seawater conditions were similar
359 between the control and experiment tanks, we note that these cases are not entirely comparable after the termination
360 of cross-pumping between tanks and the subsequent addition of alkalinity. While tanks were initially bleached,
361 eventually some biological growth was noted in each tank with potential differences in spatial and temporal
362 distribution as well as species and community differences. Herein, we assume that differences between the control
363 and experiment cases are due to the addition of alkalinity alone, but we note that characterization of other potential
364 confounding factors is a subject for future work.

365 The initial pH_T , TA, and DIC varied across experiments as seawater was collected between March 2022 and May
366 2023, ranging from pH 7.66 (December 2022) – 7.95 (May 2023), TA 2001 (May 2023) – 2176 (March 2023)
367 $\mu\text{mol}/\text{kg}$, and DIC 1847 (May 2023) – 2021 (March 2023) $\mu\text{mol}/\text{kg}$. Both measured and CO2SYS -calculated DIC
368 and TA values were normalized to salinity to account for evaporation, which drove salinity increases ranging from
369 0.2 – 7.1 across these experiments.

370 After the addition of NaOH, the control and experiment tanks were allowed to equilibrate with atmospheric CO_2 .
371 While refinements in the experimental design allowed for complete or near-complete equilibration in later
372 experiments, as determined by the stabilization of nDIC at some asymptotic value, early experiments were
373 terminated before full equilibration. In all experiments, the absorption of atmospheric CO_2 began immediately after
374 the NaOH addition, as determined by decreasing pH and Ω_{arag} and increasing DIC and seawater $p\text{CO}_2$. nTA was
375 fairly stable or increasing (+10 - 60 $\mu\text{mol kg}^{-1}$) after the NaOH addition in all cases except the $\text{pH}_T = 10.3$
376 experiment, where nTA and DIC rapidly decreased due to runaway CaCO_3 precipitation. A stable TA value is an
377 indicator that no significant persistent mineral precipitation (e.g., $\text{Mg}(\text{OH})_2$ or CaCO_3) has occurred. In the absence
378 of active mixing or bubbling, $\text{Mg}(\text{OH})_2$ precipitation occurred immediately upon the introduction of NaOH to
379 seawater, however the precipitation can be rapidly dissolved by turbulence (i.e., pumping NaOH directly above a
380 strong circulation pump and/or stream of air bubbles). No CaCO_3 precipitation was observed in the tanks or aquaria
381 for which the bulk seawater pH_T was <10.0 . The $\text{pH}_T = 10.3$ experiment was designed to induce CaCO_3 runaway
382 precipitation, as described in Section 3.3.

383 Ω_{arag} ranged from 1.4 - 2.5 in the control tanks with minimal variation over the course of any given experiment.
384 During the three experiments in which bulk pH_T was increased to ~ 8.5 , Ω_{arag} increased immediately to 6.0 - 6.3 at the
385 peak of the experiments, before slowly decreasing to 2.8 - 3.0 as the seawater equilibrated with atmospheric CO_2 .
386 For the bulk $\text{pH}_T 9.5$ experiment, Ω_{arag} increased to 20.2 and slowly decreased to 5.0 when the experiment was
387 ended at full equilibration. Mineral precipitation was observed in the bulk $\text{pH}_T 10.3$ experiment, where Ω_{arag} was
388 increased to 30.3 and rapidly (<1 week) fell to 5.2 after the addition of NaOH.

389 The results of one representative set of time-series measurements from the control and experiment tanks are shown
390 in Figure 2 for the case where pH_T of the bulk experiment tank was raised to 8.5 then allowed to relax into
391 equilibration with the atmosphere without the addition of surface air forcing or bubbling. Time-series plots for the
392 other tank-scale experiments are available in the Supplementary Materials.



394

395 **Figure 2:** Time-series data for the case where pH_T of the bulk experiment tank was raised to 8.5 with no forced air
 396 flow and no bubbling (still surface) for control (blue, solid) and experiment (red, dashed) tanks: (a) continuously
 397 measured air temperature, (b) atmospheric $p\text{CO}_2$, (c) seawater temperature, (d) salinity, and (e) dissolved oxygen; (f)
 398 pH_T measured by the SAMI-pH (circles) and interpolated from the spec-pH (line), corrected to bottle sample and
 399 CRM data; (g) NOAA/PMEL-measured TA and (h) DIC from bottle samples and normalized to salinity; (i)
 400 seawater $p\text{CO}_2$ and (j) saturation state of aragonite (Ω_{arag}) calculated from interpolated nDIC and nTA data via
 401 CO2SYS; (k) the observed carbon uptake ratio (CAR) as $(n\text{DIC}_{\text{exp}} - n\text{DIC}_{\text{control}}) / \Delta\text{TA}_{\text{NaOH addition}}$ (solid) and the
 402 theoretical CAR (dashed) from a CO2SYS calculation using measured TA and the average $p\text{CO}_2_{\text{atm}}$ to estimate the
 403 equilibrium change in DIC (dashed); (l) the percent equilibration estimated between the observed and theoretical
 404 CAR. Data gaps in panels a, b, and e are due to connectivity issues while offloading sensor data.

405 The $\Delta n\text{TA}$ and $\Delta n\text{DIC}$ values calculated between the control and experiment tanks are summarized in Figure
 406 3 where nTA and nDIC were interpolated between bottle samples measured at NOAA-PMEL, and/or were calculated
 407 via CO2SYS using sensor pH_T and TA measured at Stony Brook University corrected to less frequent NOAA-
 408 PMEL TA and DIC bottle samples. The ratio of the $\Delta n\text{DIC}$ to the addition of alkalinity in the form of NaOH, or
 409 $\Delta n\text{TA}$, is included in Figure 3 for all experiments except that of the bulk pH_T increase to 10.3. Neglecting
 410 experiments that were terminated before full equilibration, the final observed CAR ranged from 0.75 ± 0.04 to 0.87
 411 ± 0.08 (Table 1).

412 An anomalous event was noted in both the experiment and control cases for the target pH_T 8.5 experiment with
 413 forced air movement across the surface of the tank, wherein an increase in TA and DIC was noted around day 30 of
 414 the experiment. The cause of this event is unclear but could include biological changes in both tanks, the
 415 introduction of alkalinity from environmental contaminants, or the anomalous delayed release of alkalinity from
 416 suspended solids. This event was not observed in any other case, and highlights the importance of using controls to
 417 understand complex interactions in these experiments. A time-series including this event is available in the
 418 Supplementary Materials.

419 Henry's law and CO2SYS calculations were used to estimate the initial and final equilibration condition of each
 420 tank experiment. LiCOR $p\text{CO}_{2,\text{atm}}$ measurements were averaged across experiments to a representative value of 421
 421 ± 14 ppm, which was used with the initial seawater temperature and salinity to estimate $p\text{CO}_{2,\text{seawater}}$ at the beginning
 422 of each experiment. This initial $p\text{CO}_{2,\text{seawater}}$ was in all cases greater than the atmospheric $p\text{CO}_{2,\text{seawater}}$, indicating
 423 that the seawater was not fully equilibrated with the atmosphere at the time when NaOH was added, likely due to
 424 respiration and decomposition of biology removed during the bleaching step (Section 2.1), and as such, the tanks
 425 should outgas CO_2 . The initial equilibrium DIC was estimated from a CO2SYS calculation using the $p\text{CO}_{2,\text{seawater}}$
 426 and $n\text{TA}_i$, which in all cases was less than the initial $n\text{DIC}$ measured or calculated from $n\text{TA}_i$ and $\text{pH}_{T,i}$ (by 29 – 108
 427 $\mu\text{mol kg}^{-1}$). These observations underscore the importance of having a control tank to capture natural dynamics of
 428 CO_2 ingassing and outgassing to ensure that changes in DIC attributed to OAE are correctly accounted for.

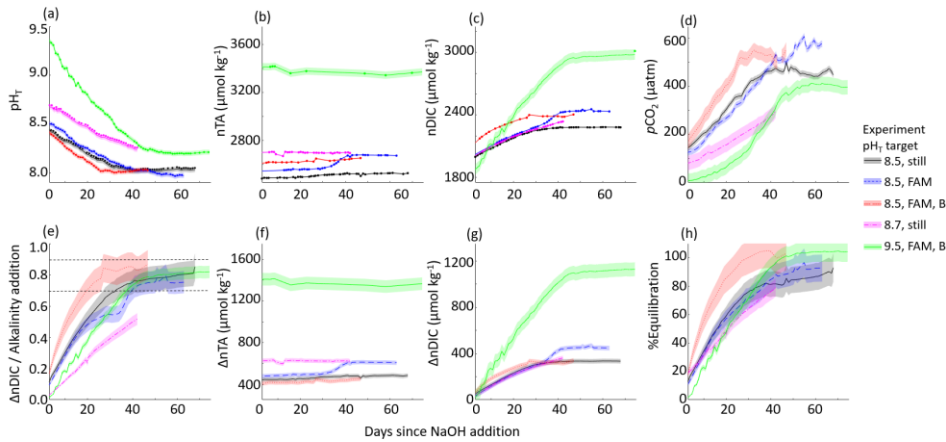
429 The final equilibrium $n\text{DIC}$ was estimated from a CO2SYS calculation using the same $p\text{CO}_{2,\text{seawater}}$ and the $n\text{TA}$
 430 measured just after the NaOH addition, corrected for the linear increase in salinity over the course of the experiment.
 431 The ratio of the expected $\Delta n\text{DIC}$ calculated at equilibrium with the atmosphere to the addition of alkalinity provides
 432 a simple estimate of the expected CO_2 storage capacity for a given experiment. The percent equilibration for each
 433 experiment was then estimated from the measured and expected values for CAR. Within the series of experiments
 434 with a targeted pH_T of 8.5, the timeline to reach an estimated 90% CO_2 equilibration decreased from 65 days (with
 435 internal circulation but still water at the surface of the tank), to 50 days (with the addition of forced air movement
 436 across the surface of the tank) to 22 days (with the addition of air bubbling). We note that only the two cases
 437 (targeted pH_T of 8.5 and 9.5) with the addition of air bubbling reached full equilibration with the atmosphere.

438 **Table 1:** Range of variables measured, calculated, or extrapolated in large tank experiments, where M denotes direct
 439 measurement, C denotes calculation via CO2SYS, and E denotes extrapolation to equilibrium conditions. Subscripts
 440 i and f refer to initial and final conditions, and 'peak' refers to the time point immediately after the addition of
 441 NaOH.

pH target	-	8.5		8.5		8.5		8.7		9.5		10.3	
Surface condition	-	Still		Forced Air		Forced Air and Air Bubbles		Still		Forced Air and Air Bubbles		Still	
Tank (C = control, E = experiment)	-	C	E	C	E	C	E	C	E	C	E	C	E
$\Delta\text{TA} = \text{NaOH addition}$ ($\pm 10 \mu\text{mol/kg}$)	M	0	409	0	462	0	375	0	626	0	1406	0	3305
Salinity _i (g/kg)	M	28.7	28.7	30.2	30.2	30.4	30.4	26.9	26.8	26.9	26.9	28.5	28.4
Salinity _f (g/kg)	M	30.5	30.2	37.3	36.6	34.7	33.7	27.6	27.6	29.0	29.2	28.6	28.6
$\text{pH}_{T,i}$ (± 0.005)	M	7.76	7.76	7.73	7.73	7.93	7.93	7.92	7.75	7.95	7.95	7.70	7.75
$\text{pH}_{T,\text{peak}}$ (± 0.005)	M	-	8.54	-	8.58	-	8.49	-	8.68	-	9.51	-	10.10
$\text{pH}_{T,f}$ (± 0.005)	M	7.88	8.05	7.85	7.99	7.99	8.01	7.84	8.26	8.01	8.21	7.75	9.52
$n\text{TA}_i$ ($\pm 10 \mu\text{mol/kg}$)	M	2049	2049	2069	2069	2248	2248	2075	2075	2007	2007	2023	2025
$n\text{TA}_{\text{peak}}$ ($\pm 10 \mu\text{mol/kg}$)	M	-	2458	-	2531	-	2623	-	2701	-	3414	-	5330
$n\text{TA}_f$ ($\pm 10 \mu\text{mol/kg}$)	M	2080	2528	2235	2674	2246	2624	2095	2696	2014	3363	2041	1253
$n\text{DIC}_i$ ($\mu\text{mol/kg}$)	M	1944	1947	1957	1996	2082	2087	1897	1975	1852	1852	1928	1938
$n\text{DIC}_f$ ($\mu\text{mol/kg}$)	M	1908	2280	2084	2433	2027	2365	1937	2336	1832	2977	1947	720
$\Omega_{\text{aragonite},i}$	C	1.39	1.37	1.4	1.1	2.0	2.0	2.4	2.4	1.9	1.9	1.4	1.3
$\Omega_{\text{aragonite},\text{peak}}$	C	-	5.9	-	6.0	-	6.2	-	8.8	-	19.3	-	30.3

$\Omega_{\text{aragonite},f}$	C	2.0	3.0	1.7	2.8	2.5	3.0	1.9	4.4	2.1	4.9	1.4	5.2
CAR_f	C	-	0.85 ± 0.04	-	0.75 ± 0.04	-	0.87 ± 0.08	-	0.52 ± 0.07	-	0.82 ± 0.09	-	-
$\text{CAR}_{\text{equilibrium}}$	E	-	0.89	-	0.85	-	0.85	-	0.84	-	0.81	-	-
% equilibration (time elapsed in days)	E	-	95 ± 10 (67)	-	92 ± 10 (63)	-	102 ± 12 (45)	-	79 ± 6 (42)	-	104 ± 7 (74)	-	(13)

442



443

444 **Figure 3:** Results of 5 tank-scale experiments in which enough NaOH was added to each tank to raise the bulk pH_T
 445 to 8.3 – 9.7. pH_T decreased rapidly in all cases in which air bubbling sped equilibration with atmospheric CO_2 .
 446 Results include: (a) measured pH_T , (b) measured nTA, (c) measured nDIC or CO2SYS calculated (for pH_T 9.5 case
 447 only), (d) CO2SYS -calculated pCO_2 , (e) the observed carbon uptake ratio (CAR) as $(\text{nDIC}_{\text{exp}} - \text{nDIC}_{\text{control}}) /$
 448 $\Delta\text{nTA}_{\text{NaOH addition}}$ with horizontal dashed lines representing the expected range of 0.7-0.9 mol CO_2 uptake / mol NaOH
 449 added to seawater, the change in (f) nTA and (g) nDIC compared to the baseline measurements before the addition
 450 of NaOH, and the percent equilibration estimated between the observed and theoretical CAR.

451 **3.2 Aquaria experiments**

452 *The large volume of tank experiments allowed for precise measurement of the seawater carbonate chemistry via*
 453 *bottle sampling (1L each, sent to NOAA/PMEL for analysis) with high sampling frequency. To compliment these*
 454 *measurements, we also performed a series of experiments in smaller aquaria (15 L each), which enabled a larger*
 455 *number of replicates and a faster time to equilibrium when bubbled with air.* Table 2 provides a summary of the
 456 range of oceanographic variables quantified for the aquaria experiments.

457 **Table 2:** Range of variables measured, calculated, or extrapolated in aquaria experiments, where M denotes direct
 458 measurement, C denotes calculation via CO2SYS, and E denotes estimation within specified equilibration
 459 conditions. Subscripts i and f refer to initial and final conditions, and ‘peak’ refers to the time point immediately
 460 after the addition of NaOH.

pH target	-	0 Control	8.3	8.5	8.5 Without air bubbles	8.7	9.3	9.5	9.7	9.9	10.0	10.1	10.2	10.3
-----------	---	-----------	-----	-----	-------------------------	-----	-----	-----	-----	-----	------	------	------	------

$\Delta TA = \text{NaOH}$ addition (± 10 $\mu\text{mol/kg}$)	M	0	187	331	362	543	1409	1679	2037	2216	2276	2504	2796	3829
$\text{pH}_{T,i}$ (± 0.1)	M	7.94	7.97	7.90	7.86	7.95	7.98	7.98	7.98	8.06	8.04	8.04	8.04	7.95
$\text{pH}_{T,\text{peak}}$ (± 0.1)	M	-	8.28	8.41	8.40	8.63	9.22	9.43	9.64	9.83	9.91	10.23	10.32	10.20
$\text{pH}_{T,f}$ (± 0.1)	M	8.06	8.03	8.07	8.11	8.08	8.21	8.20	8.23	8.65	8.96	8.72	9.46	7.99
TA_i (± 10 $\mu\text{mol/kg}$)	M	2265	2262	2250	2250	2250	2393	2393	2393	2531	2531	2531	2531	2250
TA_{peak} (± 10 $\mu\text{mol/kg}$)	M	-	2449	2582	2611	2793	3801	4072	4430	4748	-	-	-	4608
TA_f (± 10 $\mu\text{mol/kg}$)	M	2323	2476	2640	2645	2822	3837	4110	4420	4462	1702	1835	1537	2202
DIC_i ($\mu\text{mol/kg}$)	C	2089	2073	2091	2107	2070	2192	2192	2192	2282	2287	2287	2287	2067
DIC_f ($\mu\text{mol/kg}$)	C	2113	2246	2377	2382	2540	3372	3486	3877	3389	992	1244	671	2003
$\Omega_{\text{aragonite},i}$	C	2.1	2.2	1.9	1.8	2.1	2.34	2.4	2.4	2.9	2.8	2.8	2.8	2.1
$\Omega_{\text{aragonite},\text{peak}}$	C	-	4.2	5.5	5.5	8.1	19.5	23.1	27.0	29.8	30.2	30.9	32.4	38.9
$\Omega_{\text{aragonite},f}$	C	2.4	2.7	3.1	3.1	3.4	5.9	7.9	7.1	13.7	6.5	5.7	7.0	2.2
CAR_f	C	-	0.92 ± 0.10	0.87 ± 0.06	0.76 ± 0.05	0.87 ± 0.04	0.84 ± 0.02	0.86 ± 0.02	0.84 ± 0.02	0.50	-	-	-	-
$\text{CAR}_{\text{equilibrium}}$	E	-	0.69	0.67	0.64	0.77	0.80	0.80	0.80	0.81	-	-	-	-
% equilibration (time elapsed in days)	E	(40)	130 (16)	126 (18)	116 (40)	111 (16)	104 (18)	106 (18)	104 (18)	62 (1)	(1)	(1)	(1)	(16)
CaCO_3 precipitation?	M	-	No	No	No	No	No	No	No	No	Yes	Yes	Yes	Yes

461 The aquaria experiments are not directly comparable to the control stated in Table 2. Seawater for one control
462 aquarium was collected in March 2023, and was monitored for pH_T and TA changes through May 2023. Seawater
463 for the experimental aquaria was collected in three batches between March, April, and May 2023, with only 4-6
464 aquaria experiments running in parallel within each set of experiments due to space and analytical throughput
465 constraints. Because of this, the experiments started in March 2023 could be compared directly to the control (target
466 pH_T 8.3, 8.5, 8.5 still, and 8.7), but the rest of the experiments used different initial seawater than the control
467 aquaria. The CAR for each aquaria experiment was therefore calculated from changes in DIC and TA between
468 the initial ‘baseline’ condition and after the NaOH was added within a given aquarium, rather than between the
469 experiment and control cases. The CAR ranged between 0.76 ± 0.05 and 0.92 ± 0.10 , excluding cases where mineral
470 precipitation was evident and for the pH_T 9.9 case where the experiment ended after one day due to a sensor logging
471 failure. This wide range in $\Delta\text{DIC}/\Delta\text{TA}$ is likely due to the limited number of TA samples collected throughout these
472 experiments (daily at best with no duplicates due to the limited volume), and the imprecision of electrode-based pH_T
473 measurements relative to the SAMI-pH and spec-pH based measurements used in the large tank experiments.

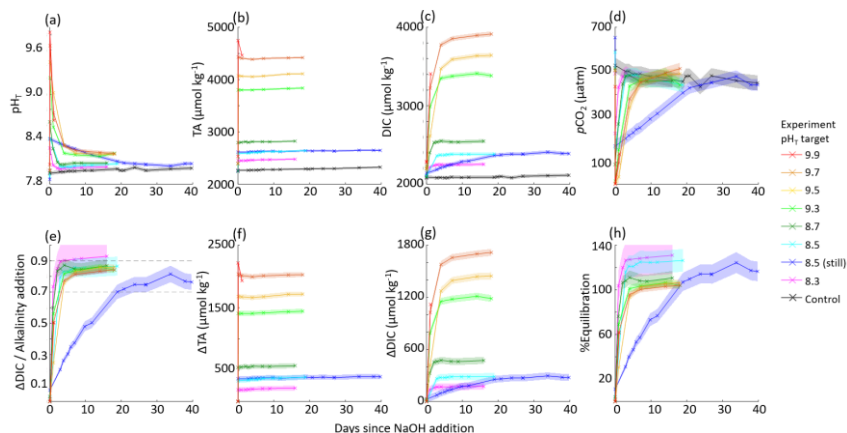
474 ~~With the exception of a single target pH_T 8.5 experiment, all aquaria were bubbled with ambient air, allowing for~~
475 ~~rapid CO_2 exchange, and an optically clear lid was placed on each aquarium to reduce evaporation and splashing~~
476 ~~onto nearby equipment. Some evaporation was evident from the rising TA throughout these experiments, but was~~
477 ~~not resolvable within the resolution of a handheld salinometer used for these experiments. No significant changes in~~
478 ~~salinity were recorded during these experiments as measured by a handheld salinometer with a range of, which~~
479 ~~ranged from values of 30 - 31 during the experiments.~~ Therefore, DIC and TA were not normalized to salinity in
480 these cases. Temperature was discretely recorded from a combination Ross pH electrode, and temperature values
481 ranged from 19 - 21 °C during the experiments.

482 ~~After the addition of NaOH, the aquaria were allowed to equilibrate with atmospheric CO_2 .~~ Similar to the large tank
483 experiments, we used Henry’s law and CO2SYS calculations to estimate the initial and final equilibration condition
484 of each aquaria experiment. The same average $p\text{CO}_{2,\text{atm}}$ of 421 ± 14 ppm was used with the initial seawater

485 temperature and salinity to estimate $p\text{CO}_{2,\text{seawater}}$ at the beginning of each experiment. The initial equilibrium DIC
 486 was estimated from a CO2SYS calculation using this $p\text{CO}_{2,\text{seawater}}$ and TA_i , which in all cases was less than the initial
 487 DIC calculated from TA_i and $\text{pH}_{T,i}$ (by $16 - 36 \mu\text{mol kg}^{-1}$). This indicates that the seawater was not fully equilibrated
 488 with the atmosphere at the time when NaOH was added, likely due to respiration and decomposition of biology
 489 removed during the bleaching step (Section 2.1), and as such, the aquaria should outgas CO_2 . The final equilibrium
 490 DIC was estimated from a CO2SYS calculation using the same $p\text{CO}_{2,\text{seawater}}$ and the TA measured just after the
 491 NaOH addition. The percent equilibration for each experiment was then estimated between the measured and
 492 predicted values for $\Delta\text{DIC} / \Delta\text{TA}$. Due to the air bubbling, most experiments approached equilibrium with the
 493 atmosphere within 1-7 days, with the exception of the non-bubbled pH_T 8.5 experiment that took ~20 days. The
 494 surface water of this non-bubbled experiment was stagnant, and the water was only mixed via stirring just before
 495 taking pH and TA samples. Absorption of atmospheric CO_2 began immediately after the NaOH addition, as
 496 determined by decreasing pH_T . We note that there are significant uncertainties in these equilibrium estimates leading to
 497 estimates of >100% equilibration. These estimates would be better constrained with more continuous carbonate
 498 chemistry measurements, particularly seawater and atmosphere $p\text{CO}_2$ throughout the experiments that would allow
 499 for more direct calculation of air-sea CO_2 flux and equilibration, and finer control of bubbling and diffusion rates are
 500 necessary to define the timeline for equilibration within the aquaria.

501 Each aquarium was gently stirred during the addition of NaOH to prevent and/or redissolve $\text{Mg}(\text{OH})_2$ precipitation.
 502 No CaCO_3 precipitation was observed in the tanks below a bulk seawater pH_T of 10.0, and TA remained stable in
 503 each of these experiments with the exception of some increase driven by minor evaporation on the order of +2
 504 $\mu\text{mol/kg}$ per day. Experiments where CaCO_3 precipitation was induced by increasing the starting pH to values above
 505 10 are discussed in Section 3.3.

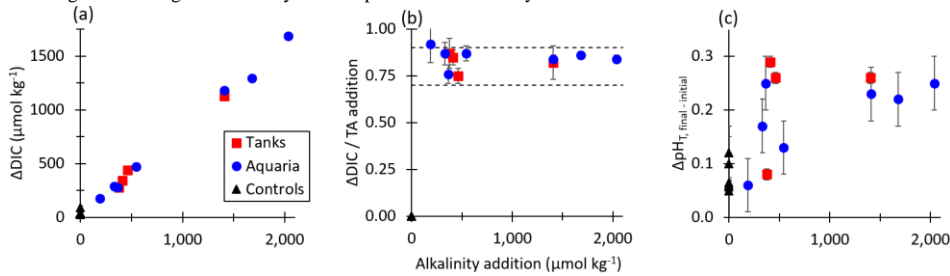
506 The aquaria experiments with target pH_T from 8.3 – 9.9 are summarized in Figure 4.



507
 508 **Figure 4:** Results of 9 aquaria experiments in which enough NaOH was added to each aquaria to raise the bulk pH_T
 509 to 8.3 – 9.9. pH_T decreased rapidly in all cases in which air bubbling sped equilibration with atmospheric CO_2 .
 510 Results include: (a) measured pH_T , (b) measured TA, (c) CO2SYS-calculated DIC, (d) CO2SYS-calculated $p\text{CO}_2$,
 511 (e) the observed carbon uptake ratio (CAR) as $(\text{DIC}_{\text{exp}} - \text{DIC}_{\text{baseline}}) / \Delta\text{TA}_{\text{NaOH addition}}$ with horizontal dashed lines
 512 representing the expected range of 0.7-0.9 mol CO_2 uptake / mol NaOH added to seawater, the change in (f) TA and
 513 (g) DIC compared to the baseline measurements before the addition of NaOH, and the percent equilibration
 514 estimated between the observed and theoretical CAR.

515 In general, the large tanks and aquaria showed reasonable agreement in achieving values for CAR within the
 516 expected range of 0.7-0.9 (He and Tyka, 2023; Burt et al., 2021; Wang et al., 2023). While the use of aquaria
 517 bubbled with air to speed equilibration allowed for a greater range of data collection within a constrained experiment
 518 timeline, the quality of this data is limited by the lack of appropriate sensors to fit into these small 15 L aquaria and
 519 fewer bottle samples due to the reduced quantity of seawater. However, while the large tanks allow for a larger
 520 range of oceanographic sampling and sensing techniques, it is more challenging to fully quantify mixing and
 521 circulation rates in the current large tank experimental setup.

522 Figure 5 shows the dependence of the equilibrium values of ΔDIC , CAR, and $\Delta\text{pH}_T = (\text{pH}_{\text{final}} - \text{pH}_{\text{initial}})$ as a function
 523 of the alkalinity addition for both tank and aquaria experiments in which the final percent equilibration for CO_2 was
 524 estimated at greater than 90%. Results for tank and aquaria experiments aligned well, with increasing ΔDIC for
 525 increasing alkalinity additions. The CAR was observed for all experiments to fall within the range expected for
 526 seawater with the temperature and salinity values used in these tests. As expected from calculations of the response
 527 of the seawater carbonate buffer system to additions of alkalinity, the pH_T at equilibrium exceeded the initial pH_T
 528 value prior to the addition of alkalinity. That is, even once equilibrium in the alkalinity enhanced experiment tank
 529 had been reached, the ending pH value was slightly elevated relative to the starting pH value. This finding warrants
 530 further investigation on the potential of OAE to mitigate some acidification impacts in controlled field trials by
 531 metering the discharge of alkalinity to semi-protected water body.



532 **Figure 5:** (a) The change in final CO2SYS-predicted DIC relative to the initial conditions for tank, aquaria, and
 533 control experiments increases with increasing NaOH additions for cases where the air-sea CO_2 equilibration was
 534 estimated at $>90\%$ at the termination of each experiment. (b) CO2SYS-predicted CAR ($\Delta\text{DIC} / \text{Alkalinity addition}$)
 535 at air-sea equilibrium conditions for tank, aquaria, and control experiments, with horizontal dashed lines
 536 representing the expected range of 0.7-0.9 mol CO_2 uptake / mol NaOH added to seawater. (c) The measured ΔpH_T
 537 $= (\text{pH}_{\text{final}} - \text{pH}_{\text{initial}})$ increases with
 538

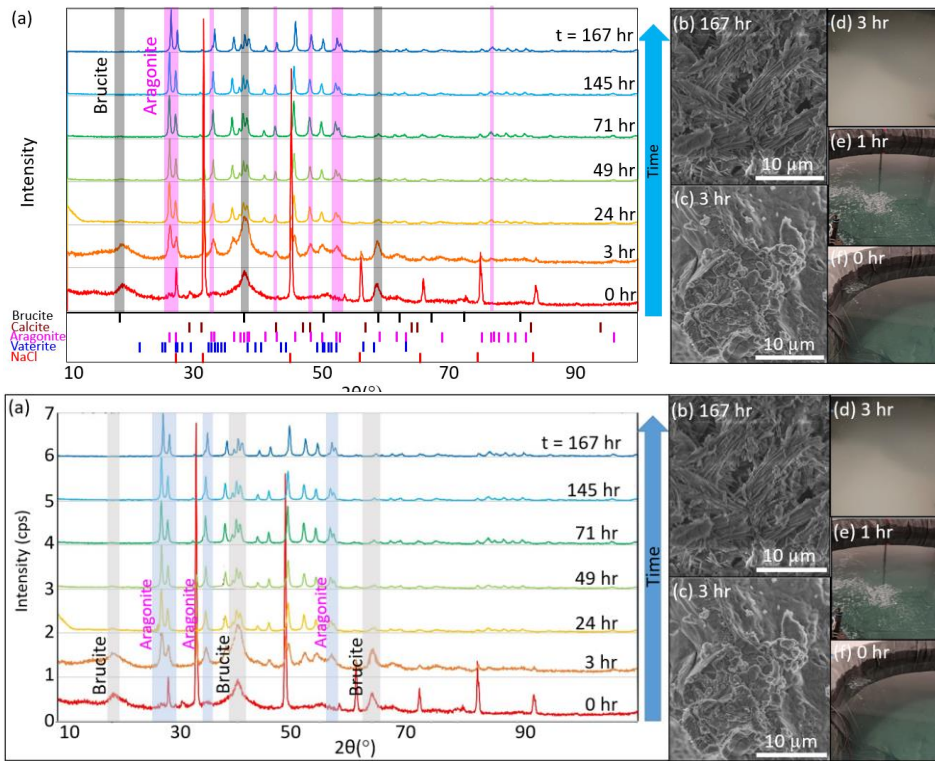
539 alkalinity addition for both tank and aquaria experiments.

540 3.3 Experiments exceeding the CaCO_3 precipitation threshold

541 While $\text{Mg}(\text{OH})_2$ precipitation occurs immediately upon introduction of concentrated (i.e., ~ 0.5 M) NaOH to still
 542 seawater, it may be rapidly dissolved or avoided entirely by gentle mixing, including via the use of stirrers,
 543 circulation pumps, or air bubblers. This precipitation and redissolution happened rapidly enough that it was not
 544 identified in any TA or other variables measured in the aquaria and tank tests. However, in cases where enough
 545 NaOH was added to raise the bulk seawater pH_T to greater than 10.0 (i.e. in one large tank test with a target pH_T of
 546 10.3, and in 4 aquaria experiments ranging from pH_T 10.0-10.3), runaway precipitation of $\text{Mg}(\text{OH})_2$ and CaCO_3 was
 547 observed. This was characterized by a sharp reduction in both TA and DIC and an increase in turbidity. Runaway
 548 precipitation has been described as a condition in which more alkalinity is removed from seawater by mineral
 549 precipitation than was initially added until a new steady state is achieved (Moras et al., 2022; Hartmann et al., 2023;

550 Suitner et al., 2023). This can significantly impact the efficiency of OAE, and has implications for biological
551 productivity, as increased turbidity may impact photosynthesis or predator-prey interactions.

552 In both the tank and aquarium pH_T 10.3 cases, discrete samples of the precipitate were collected at seven different
553 times after the bulk pH_T value reached 10.3 (0h, 3h, 24h, 49h, 71h, 145h, 167h - see Fig. 6) for XRD and SEM
554 analysis. At each timepoint, 0.5 – 1 L seawater was collected from the tank sampling port or from the center of the
555 aquaria. In cases where precipitation had visibly settled at the bottom of the aquaria, this material was stirred into the
556 water column before sampling. We note that material that settled to the bottom of the large tanks was not directly
557 collected, and that only a subset of precipitation was collected at each time point, such that later timepoints may
558 include solids that had precipitated at the beginning of the experiment. The filtered seawater was immediately
559 analyzed for TA and pH via Ross electrode because the heightened pH was out of the range of spectrophotometric
560 methods. Bottle samples of filtered seawater were not able to be analyzed at NOAA PMEL due to the continued
561 precipitation of CaCO₃ after filtration and preservation. Both XRD and SEM results showed the dominance of
562 Mg(OH)₂ precipitation immediately after the alkalinity addition and the corresponding increase in pH and Ω_{aragonite}
563 (to a value of around 30), ~~though this signal was partially obscured by the presence of other salts.~~ The Mg(OH)₂
564 precipitation at this stage was thick, slurry-like, and difficult to appropriately rinse. Broad peaks associated with
565 brucite in the 0 and 3 hr time points may reflect that these signals were partially obscured by the presence of other
566 salts, and a sharp peak in the 0 hr time point ~27° 2θ is likely associated with NaCl. Within hours of the NaOH
567 addition, the runaway CaCO₃ precipitation began, characterized by fine, light particulates in the water column and a
568 sharp increase in turbidity. Within ~24 hours of the NaOH addition, most Mg(OH)₂ signals had disappeared, leaving
569 only aragonite and calcite peaks in the XRD. The results of the XRD analysis for the tank experiment are
570 summarized in Figure 7, and the aquarium experiment showed similar results ([see Supplementary Materials](#)). TA
571 decreased throughout the precipitation of Mg(OH)₂ and CaCO₃, and was below that of the initial seawater within 24
572 hours of the NaOH addition. In the tank experiment, the initial TA (2025 μmol/kg) was raised by 3305 μmol/kg.
573 Within 3 days the TA had decreased to 1583 μmol/kg and continued to decrease through the termination of the
574 experiment to 1253 μmol/kg 10 days after the addition of NaOH. The DIC, which was initially measured at 1938
575 μmol/kg, decreased to 720 μmol/kg by the end of the experiment. This experiment shows that runaway CaCO₃ can
576 result in a significant loss of both efficiency of alkalinity dosing for OAE projects and of storage of carbon in the
577 form of DIC. A figure of time-series data collected during the tank experiment is available in the Supplementary
578 Materials.



579

580

581 **Figure 6:** (a) XRD analysis (top) of particulates filtered from seawater after the addition of enough NaOH to raise
 582 the bulk seawater pH_T to 10.3 showed mineral precipitation initially dominated by $\text{Mg}(\text{OH})_2$ before it was overtaken
 583 by $\text{CaCO}_{3,\text{arag}}$. The shaded grey vertical bars highlight several peaks characteristic of brucite which typically
 584 disappear after 24 hours, and the shaded blue bars represent several aragonite peaks which appear between 3 and 24
 585 hours after the NaOH addition. Representative SEM images show (b) $\text{CaCO}_{3,\text{arag}}$ at the end of the experiment, and (c) $\text{Mg}(\text{OH})_2$ captured ~3
 586 hours after the NaOH addition. Photographs of the tank experiment show seawater (d) ~3 hours after the NaOH
 587 addition, when runaway CaCO_3 precipitation became visually apparent, (e) during NaOH addition into still water
 588 (i.e., without the use of stirrers, circulation pumps, or air bubblers to break up and redissolve $\text{Mg}(\text{OH})_2$), and (f)
 589 before NaOH addition.

590 In summary, the presence and duration of brucite precipitation upon addition of 0.5 M aqueous NaOH depends on
 591 the ratio of the NaOH addition rate to the local dilution rate in the receiving waters. Future research using flow
 592 through tanks could help identify thresholds below which brucite precipitation can be avoided or limited, and the
 593 immediate formation of $\text{Mg}(\text{OH})_2$ may be reversible, as also noted by Suitner et al. (2023) and Cyronak et al.
 594 (2023). At the given initial seawater conditions, the threshold for aragonite precipitation began at an Ω_{arag} of 30,
 595 corresponding to $\text{pH}_T > 10.0$, and continued as Ω_{arag} decreased to ~5.2. This threshold corresponded to an increase in
 596 TA of $>2270 \mu\text{mol/kg}$. The potential for runaway aragonite-precipitation may be reduced by active mixing at the
 597 point of NaOH introduction, maintaining a mixing volume below bulk seawater pH_T of 10.0, and allowing for

598 appropriate dilution in flow-through conditions, particularly on timescales of hours after alkalinity addition.
599 Additional characterization of runaway precipitation thresholds at varying temperatures, salinities, and suspended
600 particulate conditions will allow for OAE implementation designs that best avoid this potential risk to OAE
601 efficiency and ecosystem perturbation. We note that these results are only valid for experiments that are open to the
602 atmosphere allowing for exchange of CO₂ across the air-sea boundary using an aqueous hydroxide feedstock for
603 alkalinity, and are not comparable to experiments such as closed bottle incubations, where sustained conditions of
604 high Ω_{arag} may result in precipitation at different thresholds. We also note that we do not assume zero aragonite
605 precipitation at conditions below the stated thresholds, but that potential precipitation is not readily detectable with
606 our experimental setup. For example, heterogeneous CaCO₃ precipitation events, such as may occur on suspended
607 sediments in the water column, have been suggested through characteristic changes in seawater TA/DIC ratios in
608 cases of riverine inputs and bottom sediment resuspension (Bustos-Serrano et al., 2009; Wurgaft et al., 2016; 2021).
609 Suspended sediments in the context of OAE project sites could influence OAE efficiency and the potential for
610 runaway precipitation and should be included in future studies (Bach, 2023). The thresholds determined in this study
611 are significantly higher than those of some mineral-based OAE studies, including precipitation after an increase in
612 TA of ~500 $\mu\text{mol/kg}$ using CaO and Ca(OH)₂ mineral additions (Moras et al., 2022). Hartmann et al. (2022) noted
613 precipitation resulting from alkalinity additions of >600 $\mu\text{mol/kg}$ Mg(OH)₂, and found that alkaline solutions
614 avoided carbonate precipitation better than reactive alkaline particle additions to seawater. Suitner et al. (2023)
615 suggested that alkalinity additions > 2000 $\mu\text{mol/kg}$ could be achievable given sufficient dilution to avoid runaway
616 precipitation. Together, these studies highlight the need to expand research into runaway precipitation to
617 characterize potential inefficiencies in OAE, particularly in in-situ experiments to establish relationships applicable
618 to ocean environments.

619 **5 Summary and Future Work**

620 These results demonstrate that ocean alkalinity enhancement using aqueous sodium hydroxide in seawater results in
621 CO₂ removal from air at an efficiency of 0.75 (\pm 0.04) – 0.92 (\pm 0.10), with 90% equilibration typically achieved
622 within 7 - 9 weeks (still surface water with ~16 L/min subsurface circulation through UV arrays) to 3 - 5 weeks
623 (with the addition of ambient air bubbling into the bottom of each tank) of the initial addition when performed in
624 ~6000 L tanks with seawater-air contact areas of around 4.6 m². These results are in general agreement with ratios
625 noted in Burt et al. (2021), He and Tyka (2023), and Wang et al., (2023). Here, uncertainties are driven by sensor
626 precision and temporal resolution in discrete DIC and TA sampling, the limited number of experiments with
627 minimal opportunities for duplicates or replicates, and poorly constrained data on mixing, circulation, and air
628 bubbling rates. Ongoing experiments seek to improve each of these conditions and should particularly focus on
629 constraining the movement of water within a given tank to improve air-sea equilibration estimates and to allow for
630 better extrapolation from tank to field experiments. In addition, a focus of ongoing and future work is to provide rate
631 estimates for the uptake of atmospheric CO₂ in response to an NaOH addition, allowing for fitting and extrapolation
632 of a shortened experiment to equilibration with the atmosphere.

633 We relied on several methods to constrain seawater carbonate chemistry. The tank-scale experiments primarily
634 relied on discrete (at most daily) DIC and TA sampling (NOAA PMEL), paired with daily measurements from
635 spectrophotometric pH systems (SAMI-pH and a semi-automated benchtop spec-pH system following Carter et al.
636 (2013)) and local TA measurements. With appropriate calibration or correction of the spec-pH systems relative to
637 CRM, there was no significant difference in carbonate calculations using the NOAA PMEL DIC-TA or spec-pH-
638 local TA pairings, though the latter case typically produced larger uncertainties. Aquaria experiments relied on a
639 standard glass pH electrode (at most daily, corrected to spectrophotometric systems) with discrete (at most daily) TA
640 measurements, which provided reasonable data relative to the tank experiments. As a result, ongoing tank-scale
641 experiments have limited the volume of discrete DIC and TA samples collected for analysis at NOAA PMEL to
642 allow for faster and less expensive monitoring via spec-pH and local TA titrations. However, we note that the major
643 limitation in this measurement pathway lies in the spec-pH method, which is typically limited to pH_T measurements

644 ranging from 7 – 9 for the meta-cresol purple indicator dye used. While our measurements retained some sensitivity
645 up to pH_T 9.5, such a method should typically be considered unreliable at these pH_T values, and we relied on
646 frequent correction to CRM and comparison with DIC/TA samples. Thymol blue is an alternative
647 spectrophotometric pH_T indicator dye with sensitivity over the higher pH_T conditions observed during these initial
648 trials and will be assessed for future experiments (Zhang and Byrne, 1996; Liu et al., 2006).

649 Aqueous NaOH with concentrations as high as 0.5 M can be added directly to turbulent seawater with only limited
650 observable precipitation of $\text{Mg}(\text{OH})_2$. In these conditions this precipitated mineral rapidly redissolves on the
651 timescales of minutes to seconds. Improved control over the NaOH dosing rate (in our tank experiments, ~50 mL
652 NaOH/min) and the turbulence of the receiving water through metered flow through experiments will be valuable in
653 extrapolating to field conditions. This precipitation is detectable both visually and through turbidity measurements
654 and implies that straightforward measurement of pH and turbidity at the dispersal site can be used to adjust the
655 alkalinity dispersal rate according to local mixing conditions such that $\text{Mg}(\text{OH})_2$ precipitation is avoided and/or
656 redissolves when it occurs. No significant CaCO_3 precipitation was observed at $\text{pH} < 10.0$ or $\Omega_{\text{aragonite}} < 30.0$.
657 Runaway CaCO_3 precipitation was observed above these thresholds, where a massive precipitation and settling of
658 $\text{Mg}(\text{OH})_2$ and CaCO_3 solids results in less alkalinity in the overlying water than at the starting condition. pH and
659 turbidity sensing combined with discrete TA measurements could be used as a feedback signal for alkalinity dosing
660 into seawater to ensure that the local maximum thresholds at the dispersal location do not approach or exceed
661 conditions that promote significant CaCO_3 precipitation. We note that future investigations seeking to better
662 approximate field conditions should take into account seasonal and tidal shifts in temperature and salinity, and
663 varying conditions of suspended sediment in the water column, including that of aerial dust, terrestrial runoff, and
664 resuspended bottom sediments.

665 In these experiments, the seawater was filtered and bleach treated prior to experiments to limit biological growth,
666 and both tank and aquaria experiments were conducted indoors with limited light. Nevertheless, in most
667 experiments, biological growth was observed after a few weeks, including cyanobacteria and coccolithophores. A
668 series of experiments are underway to test the difference in CO_2 removal efficiency for two side-by-side tanks, both
669 of which are dosed with NaOH, but only one of which was bleached. Preliminary results show minimal difference
670 between the bleached and unbleached tanks, indicating these experiments are applicable to real-world conditions, at
671 least for regions with biological communities similar to that of Long Island Sound, but further investigation is
672 warranted.

673 A focus of future work is to consider the potential impact of the SEAMATE process on local ocean acidification
674 mitigation efforts. We note that in each constrained tank and aquaria experiment, the pH_T at equilibrium exceeds
675 the initial pH_T value prior to the addition of alkalinity. A controlled release of alkalinity could theoretically be
676 configured to maintain a locally elevated pH_T value relative to pre-alkaline conditions, with potential uses in
677 aquaculture and hatchery environments.

678 These results provide clear and practical guidelines for MRV for OAE implementations employing aqueous
679 alkalinity. First, carbonate chemistry and turbidity measurements at the alkalinity dispersal location can ensure that
680 seawater parameters such as pH and $\Omega_{\text{aragonite}}$ remain within pre-determined safe bounds and that unwanted
681 precipitation is avoided. Second, for a given OAE deployment, where ocean models provide a reasonable certainty
682 about the fraction of the alkalinity plume remaining in the surface over weeks to months, the CO_2 removal efficiency
683 and timescale for air-seawater equilibration provided by our experiments can place a lower bound on the amount of
684 CO_2 removal expected from that OAE intervention. Expanding these studies from tank scale to mesocosm and field
685 experiments will be crucial to understanding biological impacts and constraining realistic air-sea interactions in
686 response to this type of OAE (Oschlies et al., 2023).

687 **Data availability**

688 Data are described in the manuscript and provided Supplementary Materials, which includes a .csv file with
689 processed sensor and sample time-series data at hourly resolution.

690 **Author contribution**

691 MDE and BRC designed the experiments and MCR carried them out with support from NH, CS, and XL. JH
692 provided support on experimental setup and instrumentation. MCR prepared the manuscript with contributions from
693 all co-authors.

694 **Competing interests**

695 MCR is Lead Oceanographer and Head of MRV at Ebb Carbon, Inc. MDE is Co-Founder and Chief Scientific
696 Advisor at Ebb Carbon, Inc.

697 **Acknowledgements**

698 We would like to than Stephen Abrams and Thomas Wilson at Stony Brook University Flax Pond Marine Lab for
699 technical assistance in experiment setup. We thank Chris Ikeda and Susan Curless of NOAA PMEL for support in
700 discrete sample analysis. We thank Mike Tyka for productive discussions. We thank Eyal Wurgaft for assistance in
701 TA titrations.

702 **Funding**

703 We acknowledge funding from The Grantham Foundation for the Protection of the Environment under the SEA
704 MATE (Safe Elevation of Alkalinity for the Mitigation of Acidification Through Electrochemistry) grant. In
705 addition, this research used the XRD facility of the Center for Functional Nanomaterials (CFN), which is a U.S.
706 Department of Energy Office of Science User Facility, at Brookhaven National Laboratory under Contract No. DE-
707 SC0012704. BRC and JH were funded through the Cooperative Institute for Climate, Ocean, and Ecosystem
708 Studies (CICOES) under NOAA Cooperative Agreement NA20OAR4320271 and supported by NOAA's PMEL.

709 **References**

- 710
711 Albright, R., Caldeira, L., Hosfelt, J., Kwiatkowski, L., Maclaren, J.K., Mason, B.M., Nebuchina, Y. et al.: Reversal
712 of ocean acidification enhances net coral reef calcification. *Nature*, 531, no. 7594: 362-365, 2016.
713 Bach, L.T.: The additionality problem of ocean alkalinity enhancement. *Biogeosciences*, 21, 261-277, 2024.
714 [Discussion- \[preprint\], in review, 2023](#)
715 Bach, L. T., Gill, S.J., Rickaby, R.E.M., Gore, S., and Renforth, P.: CO₂ removal with enhanced weathering and
716 ocean alkalinity enhancement: potential risks and co-benefits for marine pelagic ecosystems. *Frontiers in*
717 *Climate*, 1, 7, 2019.
718 Bainbridge, Z., Lewis, S., Bartley, R., Fabricius, K., Collier, C., Waterhouse, J., Garzon-Garcia, A., Robson, B.,
719 Burton, J., Wenger, A., and Brodie, J: Fine sediment and particulate organic matter: A review and case study on
720 ridge-to-reef transport, transformations, fates, and impacts on marine ecosystems. *Marine Pollution Bulletin*
721 135, pp. 1205-1220. 2018
722 Berner, R. A., Lasaga, A.C., and Garrels, R.M.: Carbonate-silicate geochemical cycle and its effect on atmospheric
723 carbon dioxide over the past 100 million years. *Am. J. Sci.:(United States)* 283, no. 7, 1983.
724 Boettcher, M., Chai, F. Cullen, J., Goeschl, T., Lampitt, R., Lenton, A., Oeschlies, A. et al.: High level review of a
725 wide range of proposed marine geoengineering techniques. *GESAMP Working Group Reports and Studies*, 41,
726 2019.
727 Broderon, K.E., Hammer, K.J., Schrameyer, V., Floytrup, A., Rasheed, M.A., Ralph, P.J., Kühl, M., and Pederson,
728 O.: Sediment resuspension and deposition on seagrass leaves impedes internal plant aeration and promotes
729 phytotoxic H₂S intrusion. *Frontiers in Plant Science* 8. 2017

730 Burt, D.J., Fröb, F., & Ilyina, T.: The sensitivity of the marine carbonate system to regional ocean alkalinity
731 enhancement. *Frontiers in Climate* 3, 624075. 2021

732 Bustos-Serrano, H., Morse, J.W., & Millero, F.J.: The formation of whittings on the Little Bahama Bank. *Marine*
733 *Chemistry* 113, no. 1-2, pp. 1-8. 2009

734 Butenschön, M., Lovato, T., Masina, S., Caserini, S., and Grosso, M.: Alkalinization scenarios in the Mediterranean
735 Sea for efficient removal of atmospheric CO₂ and the mitigation of ocean acidification. *Frontiers in Climate* 3,
736 614537. 2021

737 Carter, B. R., J. A. Radich, H. L. Doyle, and A. G. Dickson.: An automated system for spectrophotometric seawater
738 pH measurements. *Limnology and Oceanography: Methods*, 11, no. 1: 16-27, 2013.

739 Caserini, S., Storni, N., & Grosso, M.: The availability of limestone and other raw materials for ocean alkalinity
740 enhancement. *Global Biogeochemical Cycles*, 36, e2021GB007246. <https://doi.org/10.1029/2021GB007246>,
741 2022.

742 Cross, J.N., Sweeney, C., Jewett, E.B., Feely, R.A., McElhany, P., Carter, B., Stein, T., Kitch, G.D., and Gledhill,
743 D.: Strategy for NOAA carbon dioxide removal research: A white paper documenting a potential NOAA CDR
744 science strategy as an element of NOAA's Climate Interventions Portfolio. NOAA Special Report. NOAA,
745 Washington, DC. DOI: 10.25923/gzke-8730. 2023

746 Cyronak, T., Albright, R., and Bach, L.: [Field experiments in ocean alkalinity enhancement research. *State of the*](https://doi.org/10.5194/sp-2023-9)
747 [Planet, 2-oae2023 \(7\). 2023.](https://doi.org/10.5194/sp-2023-9)

748 [Chapter 4.5: Field Experiments, State Planet Discuss. \[preprint\], https://doi.org/10.5194/sp-2023-9, in review, 2023.](https://doi.org/10.5194/sp-2023-9)

749 de Lannoy, C.-F., Eisaman, M.D., Jose, A., Karnitz, S.D., DeVaul, R.W., Hannun, K., and Rivest, J.L.B.: Indirect
750 ocean capture of atmospheric CO₂: Part I. Prototype of a negative emissions technology. *International journal of*
751 *greenhouse gas control*, 70: 243-253, 2018.

752 Dickson, A. G.: An exact definition of total alkalinity and a procedure for the estimation of alkalinity and total
753 inorganic carbon from titration data. *Deep Sea Research Part A. Oceanographic Research Papers*, 28(6), 609–
754 623, 1981.

755 Dickson, A. G.: The development of the alkalinity concept in marine chemistry. *Marine Chemistry*, 40(1–2), 49–63,
756 1992.

757 Dickson, A.G.: Thermodynamics of the dissociation of boric acid in synthetic seawater from 273.15 to 318.15 K.
758 *Deep Sea Research Part A. Oceanographic Research Papers*, 37, no. 5: 755-766, 1990.

759 Dickson, A.G., Sabine, C.L., and Christian, J.R.: Guide to best practices for ocean CO₂ measurements. North Pacific
760 Marine Science Organization, 2007. Eisaman, M. D., Parajuly, K., Tuganov, A., Eldershaw, C., Chang, N.,
761 Littau, K. A. CO₂ Extraction from Seawater Using Bipolar Membrane Electrodialysis, *Energy Environ. Sci.*, 5:
762 7346. <https://doi.org/10.1039/c2ee03393c>, 2012.

763 Eisaman, M. D.; Rivest, J. L. B.; Karnitz, S. D.; De Lannoy, C.-F.; Jose, A.; DeVaul, R. W.; Hannun, K. Indirect
764 Ocean Capture of Atmospheric CO₂: Part II. Understanding the Cost of Negative Emissions. *International*
765 *Journal of Greenhouse Gas Control*, 70: 254–261, <https://doi.org/10.1016/j.ijggc.2018.02.020>, 2018.

766 Eisaman, M. D., Geilert, S., Renforth, P., Bastianini, L., Campbell, J., Dale, A. W., Foteinis, S., Grasse, P., Hawrot,
767 O., Löscher, C. R., Rau, G. H., and Rønning, J.: Assessing the technical aspects of ocean-alkalinity-
768 enhancement approaches, in: *Guide to Best Practices in Ocean Alkalinity Enhancement Research*, edited by:
769 Oschlies, A., Stevenson, A., Bach, L. T., Fennel, K., Rickaby, R. E. M., Satterfield, T., Webb, R., and Gattuso,
770 J.-P., Copernicus Publications, *State Planet, 2-oae2023, 3*, <https://doi.org/10.5194/sp-2-oae2023-3-2023>, 2023.

771 Feely, R.A., Alin, S., Carter, B., Bednaršek, N., Hales, B., Chan, F., Hill, T.M., Gaylord, B., Sanford, E., Byrne,
772 R.H., Sabine, C.L., Greeley, D., Juraneck, L., Chemical and biological impacts of ocean acidification along the
773 west coast of North America, *Estuarine, Coastal and Shelf Science*, doi: 10.1016/j.ecss.2016.08.043, 2016.

774 Feng, E. Y., Koeve, W., Keller, D.P., and Oschlies, A.: Model-Based Assessment of the CO₂ Sequestration Potential
775 of Coastal Ocean Alkalinization. *Earth's Future*, 5, no. 12: 1252-1266, 2017.

776 [Fennel, K., Long, M.C., Algar, C., Carter, B., Keller, D., Laurent, A., Mattern, J.P., Musgrave, R., Oschlies, A.,](https://doi.org/10.5194/sp-2023-10)
777 [Ostiguy, J., Palter, J.B., and Whitt, D.B.: Modeling considerations for research on Ocean Alkalinity](https://doi.org/10.5194/sp-2023-10)
778 [Enhancement \(OAE\). *State of the Planet, 2-oae2023 \(9\). 2023. Fennel, K., Long, M.-C., Algar, C., Carter, B.,*](https://doi.org/10.5194/sp-2023-10)
779 [Keller, D., Laurent, A., Mattern, J. P., Musgrave, R., Oschlies, A., Ostiguy, J., Palter, J., and Whitt, D.-B.:](https://doi.org/10.5194/sp-2023-10)
780 [Modeling considerations for research on Ocean Alkalinity Enhancement \(OAE\). *State Planet Discuss.*](https://doi.org/10.5194/sp-2023-10)
781 [\[preprint\], https://doi.org/10.5194/sp-2023-10, in review, 2023.](https://doi.org/10.5194/sp-2023-10)

782 Ferderer, A., Chase, Z., Kennedy, F., Schulz, K.G., and Bach, L.T.: Assessing the influence of ocean alkalinity
783 enhancement on a coastal phytoplankton community. *Biogeosciences* 19, no. 23: 5375-5399, 2022.

784 Friis, K.; Körtzinger, A.; Wallace, D. W. R. The Salinity Normalization of Marine Inorganic Carbon Chemistry
785 Data. *Geophys. Res. Lett.*, 30 (2). <https://doi.org/10.1029/2002GL015898>, 2003.

786 Groen, A., Kittu, L., Ortiz Cortes, J., Schulz, K., and Riebesell, U.: Assessing the response of particulate organic
787 matter stoichiometry to ocean alkanisation. Ocean Visions Summit, Atlanta, Georgia, USA,
788 2023ocvi.conf27171G, 4-6 April 2023

789 Hartmann, J., Saitner, N., Lim, C., Schneider, J., Marín-Samper, L., Arístegui, J., Renforth, P., Taucher, J., and
790 Riebesell, U.: Stability of alkalinity in ocean alkalinity enhancement (OAE) approaches—consequences for
791 durability of CO₂ storage. *Biogeosciences* 20, no. 4: 781-802, 2023.

792 Harvey, L.: Mitigating the atmospheric CO₂ increase and ocean acidification by adding limestone powder to
793 upwelling regions. *Journal of 640 Geophysical Research: Oceans*, 113, 2008.

794 He, J. and Tyka, M. D.: Limits and CO₂ equilibration of near-coast alkalinity enhancement, *Biogeosciences*, 20, 27–
795 43, <https://doi.org/10.5194/bg-20-27-2023>, 2023.

796 [Ho, D. T., Bopp, L., Palter, J. B., Long, M. C., Boyd, P. W., Neukermans, G., and Bach, L. T.: Monitoring, reporting,
797 and verification for ocean alkalinity enhancement. *State of the Planet, 2-0ae2023 \(12\)*, 2023. Ho, D. T., Bopp,
798 L., Palter, J. B., Long, M. C., Boyd, P., Neukermans, G., and Bach, L.: Chapter 6: Monitoring, Reporting, and
799 Verification for Ocean Alkalinity Enhancement, *State Planet Discuss.* \[preprint\], \[https://doi.org/10.5194/sp-
800 2023-2\]\(https://doi.org/10.5194/sp-2023-2\), in review, 2023.](https://doi.org/10.5194/sp-2023-2)

801 Ilyina, T., Wolf-Gladrow, D., Munhoven, G., and Heinze, C.: Assessing the potential of calcium-based artificial
802 ocean alkanization to mitigate rising atmospheric CO₂ and ocean acidification, *Geophysical Research Letters*,
803 40, 5909-5914, 2013.

804 IPCC: Summary for Policymakers. In: *Climate Change 2021: The Physical Science Basis, Contribution of Working
805 Group I to the Sixth Assessment Report of the Intergovernmental Panel on Climate Change*, edited by: Masson-
806 Delmotte, V., Zhai, P., Pirani, A., Connors, S. L., Péan, C., Berger, S., Caud, N., Chen, Y., Goldfarb, L., Gomis,
807 M. I., Huang, M., Leitzell, K., Lonnoy, E., Matthews, J. B. R., Maycock, T. K., Waterfield, T., Yelekçi, O., Yu,
808 R., and Zhou, B.: Cambridge University Press, Cambridge, United Kingdom and New York, NY, USA, 3–32,
809 <https://doi.org/10.1017/9781009157896.001>, 2022.

810 Isson, T. T., Planavsky, N. J., Coogan, L. A., Stewart, E. M., Ague, J. J., Bolton, E. W., et al.: Evolution of the
811 global carbon cycle and climate regulation on earth. *Global Biogeochemical Cycles*, 34, e2018GB006061,
812 <https://doi.org/10.1029/2018GB006061>, 2020.

813 Johnson, K.M., King, A.E., and Sieburth, J.M.: Coulometric TCO₂ analyses for marine studies: An introduction.
814 *Marine Chemistry* 16, pp. 61-82. 1985.

815 Jones, D.C., Ito, T., Takano, Y., and C.-W Hsu, C.-W.: Spatial and seasonal variability of the air-sea equilibration
816 timescale of carbon dioxide. *Global Biogeochemical Cycles*, 28(11), 1163–1178,
817 <https://doi.org/10.1002/2014GB004813>, 2014.

818 Khesghi, H. S.: Sequestering atmospheric carbon dioxide by increasing ocean alkalinity, *Energy*, 20, 915-922, 1995.

819 Köhler, P., Hartmann, J., and Wolf-Gladrow, D.A.: Geoengineering potential of artificially enhanced silicate
820 weathering of olivine. *Proceedings of the National Academy of Sciences* 107, no. 47: 20228-20233, 2010.

821 La Plante, E., Chen, X., Bustillos, S., Bouissonnie, A., Traynor, T., Jassby, D., Corsini, L., Simonetti, D., and Sant,
822 G.: Electrolytic seawater mineralization and the mass balances that demonstrate carbon dioxide removal. *ACS
823 EST Engg.* <https://doi.org/10.1021/acsestengg.3c00004>, 2023.

824 Lee, K., Kim, T.-W., Byrne, R.H., Millero, F.J., Feely, R.A., and Liu, Y.-M.: The universal ratio of boron to
825 chlorinity for the North Pacific and North Atlantic oceans. *Geochimica et Cosmochimica Acta* 74, no. 6: 1801-
826 1811, 2010.

827 Lewis, E., Wallace, D., & Allison, L. J.: Program developed for CO₂ system calculations.
828 <https://doi.org/10.2172/639712>, 1998.

829 Liu, X., Wang, Z.A., Byrne, R.H., Kaltenbacher, E.A., and Bernstein, R.E.: Spectrophotometric measurements of
830 pH in-situ: laboratory and field evaluations of instrumental performance. *Environmental Science & Technology*
831 40, no. 16, 5026-5044. 2006

832 Lu, X., Ringham, M., Hirtle, N., Hillis, K., Shaw, C., Herndon, J., Carter, B.R., and Eisaman, M.D.:
833 Characterization of an Electrochemical Approach to Ocean Alkalinity Enhancement. In *AGU Fall Meeting
834 Abstracts*, vol. 2022, pp. GC31C-01. 2022.

835 Lueker, T.J., Dickson, A.G., and Keeling, C.D.: Ocean pCO₂ calculated from dissolved inorganic carbon, alkalinity,
836 and equations for K₁ and K₂: validation based on laboratory measurements of CO₂ in gas and seawater at
837 equilibrium. *Marine chemistry* 70, no. 1-3: 105-119, 2000.

838 Minx, J.C., Lamb, W.F., Callaghan, M.W., Fuss, S., Hilaire, J., Creutzig, F., Amann, T., et al.: Negative
839 emissions—Part 1: Research landscape and synthesis. *Environmental Research Letters* 13, no. 6: 063001, 2018.

Field Code Changed

840 Montserrat, F., Renforth, P., Hartmann, J., Leermakers, M., Knops, P., and Meysman, F.J.R.: Olivine dissolution in
841 seawater: implications for CO₂ sequestration through enhanced weathering in coastal environments.
842 *Environmental Science & Technology* 51, no. 7: 3960-3972, 2017.

843 Moras, C.A., Bach, L.T., Cyronak, T., Joannes-Boyau, R., and Schulz, K.G.: Ocean alkalinity enhancement–
844 avoiding runaway CaCO₃ precipitation during quick and hydrated lime dissolution. *Biogeosciences* 19, no. 15:
845 3537-3557, 2022.

846 National Academies of Sciences, Engineering, and Medicine. A research strategy for ocean-based carbon dioxide
847 removal and sequestration. 2021.

848 National Academies of Sciences, Engineering, and Medicine. Negative Emissions Technologies and Reliable
849 Sequestration: A Research Agenda. 2018.

850 Nduagu, E. "Production of Mg(OH)₂ from Mg-silicate rock for CO₂ mineral sequestration. Dissertation for Abo
851 Akademi University, 2012.

852 [Oschlies, A., Bach, L., Rickaby, R., Satterfield, T., Webb, R. M., and Gattuso, J.-P.: Climate targets, carbon dioxide](#)
853 [removal and the potential role of Ocean Alkalinity Enhancement. *State of the Planet*, 2-oae2023 \(1\), 2023.](#)

854 [Oschlies, A., Bach, L., Rickaby, R., Satterfield, T., Webb, R. M., and Gattuso, J.-P.: Climate targets, carbon dioxide](#)
855 [removal and the potential role of Ocean Alkalinity Enhancement, *State Planet Discuss.* \[preprint\],](#)
856 <https://doi.org/10.5194/sp-2023-13>, in review, 2023.

857 Pierrot, D., Lewis, E., and Wallace, D.W.R.: MS Excel program developed for CO₂ system calculations.
858 ORNL/CDIAC-105a. Carbon Dioxide Information Analysis Center, Oak Ridge National Laboratory, U.S.
859 Department of Energy, Oak Ridge, Tennessee, 2006.

860 Rau, G.H.: Electrochemical splitting of calcium carbonate to increase solution alkalinity: Implications for mitigation
861 of carbon dioxide and ocean acidity. *Environmental science & technology* 42, no. 23: 8935-8940, 2008.

862 Renforth, P., and Henderson, G.: Assessing ocean alkalinity for carbon sequestration. *Reviews of Geophysics* 55,
863 no. 3: 636-674, 2017.

864 Rigopoulos, I., Harrison, A.L., Delimitis, A., Ioannou, I., Efstathiou, A.M., Kyratsi, T., and Oelkers, E.H. : Carbon
865 sequestration via enhanced weathering of peridotites and basalts in seawater. *Applied Geochemistry* 91: 197-
866 207, 2018.

867 Rueda, O., Mogollón, J.M., Tukker, A., and Scherer, L.: Negative-emissions technology portfolios to meet the 1.5°
868 C target. *Global Environmental Change* 67: 102238, 2021.

869 Rogelj, J., Popp, A., Calvin, K. V., Luderer, G., Emmerling, J., Gernaat, D., Fujimori, S., Strefler, J., Hasegawa, T.,
870 Marangoni, G., Krey, V., Kriegler, E., Riahi, K., van Vuuren, D. P., Doelman, J., Drouet, L., Edmonds, J.,
871 Fricko, O., Harmsen, M., Havlík, P., Humpenöder, F., Stehfest, E., and Tavoni, M.: Scenarios towards limiting
872 global mean temperature increase below 1.5 °C. *Nat. Clim. Change*, 8, 325–332, [https://doi.org/10.1038/s41558-](https://doi.org/10.1038/s41558-018-0091-3)
873 [018-0091-3](https://doi.org/10.1038/s41558-018-0091-3), 2018.

874 [Schulz, K. G., Bach, L. T., and Dickson, A. G.: Seawater carbonate system considerations for ocean alkalinity](#)
875 [enhancement research: theory, measurements, and calculations. *State of the Planet*, 2-oae2023 \(2\), 2023.](#)
876 [Schulz, K. G., Bach, L. T., and Dickson, A. G.: Seawater carbonate system considerations for ocean alkalinity](#)
877 [enhancement research, *State Planet Discuss.* \[preprint\], <https://doi.org/10.5194/sp-2023-12>, in review, 2023.](#)

878 Shaw, C., Ringham, M.C., Lu, X., Carter, B.R., Eisaman, M.D., and Tyka, M.: Understanding the Kinetics of
879 Electrochemically derived Magnesium Hydroxide for Ocean Alkalinity Enhancement. In AGU Fall Meeting
880 Abstracts, vol. 2022, pp. GC32I-0713. 2022.

881 Song, S., Wang, Z.A., Gonnee, M.E., Kroeger, K.D., Chu, S.N., Li, D., and Liang, H.: An important
882 biogeochemical link between organic and inorganic carbon cycling: Effects of organic alkalinity on carbonate
883 chemistry in coastal waters influenced by intertidal salt marshes. *Geochimica et Cosmochimica Acta* 275:123-
884 139, 2020.

885 Suitner, N., Faucher, G., Lim, C., Schneider, J., Moras, C.A., Riebesell, U., and Hartmann, J.: Ocean alkalinity
886 enhancement approaches and the predictability of runaway precipitation processes- Results of an experimental
887 study to determine critical alkalinity ranges for safe and sustainable application scenarios. *EGU sphere*
888 [preprint], <https://doi.org/10.5194/egusphere-20223-2611>, 2023

889 Tyka, M.D., Arsdale, C.V., and Platt, J.C.: CO₂ capture by pumping surface acidity to the deep ocean. *Energy &*
890 *Environmental Science* 15, no. 2: 786-798, 2022.

891 Van Heuven, S., Pierrot, D., Rae, J., Lewis, E., & Wallace, D.: MATLAB program developed for CO₂ system
892 calculations. ORNL/CDIAC-105b, 530, 2011.

893 Vitillo, J. G., Eisaman, M.D., Aradóttir, E.S.P., Passarini, F., Wang, T., and Sheehan, S.W.: The role of carbon
894 capture, utilization and storage for economic pathways that limit global warming to below 1.5° C." *Iscience*:
895 104237, 2022.

Field Code Changed

896 Wang, H., Pilcher, D. J., Kearney, K. A., Cross, J. N., Shugart, O. M., Eisaman, M. D., & Carter, B. R.: Simulated
897 impact of ocean alkalinity enhancement on atmospheric CO₂ removal in the Bering Sea. *Earth's Future*, 11(1),
898 e2022EF002816, 2023

899 Wang, Z. A. and Cai, W. J.: Carbon dioxide degassing and inorganic carbon export from a marsh-dominated estuary
900 (the Duplin River): A marsh CO₂ pump. *Limnol. Oceanogr.* 49, 341–354, 2004.

901 Wolf-Gladrow, D. A., Zeebe, R. E., Klaas, C., Körtzinger, A., & Dickson, A. G.: Total alkalinity: The explicit
902 conservative expression and its application to biogeochemical processes. *Marine Chemistry*, 106(1–2), 287–
903 300, 2007.

904

905 Wurgaft, E., Steiner, Z., Luz, B., and Lazar, B.: Evidence for inorganic precipitation of CaCO₃ on suspended solids
906 in the open water of the Red Sea, *Marine Chemistry*, 186, pp. 145–155, 2016.

907 Wurgaft, E., Wang, Z., Churchill, J., Dellapenna, T., Song, S., Du, J., Ringham, M., Rivlin, T., and Lazar, B.:
908 Particle triggered reactions as an important mechanism of alkalinity and inorganic carbon removal in river
909 plumes, *Geophysical Research Letters*, 48, e2021GL093178, <https://doi.org/10.1029/2021GL093178>, 2021

910 Zeebe, R.E., and Wolf-Gladrow, D.: CO₂ in seawater: equilibrium, kinetics, isotopes. Vol. 65, Gulf Professional
911 Publishing, 2001.

912 Zhang, H., and Byrne, R.H.: Spectrophotometric pH measurements of surface seawater at in-situ conditions:
913 absorbance and protonation behavior of thymol blue. *Marine Chemistry* 52, no. 1, pp. 17-25. 1996